2017

Serpentinization and Synthesis: Searching for Abiotic and Biotic Non-Volatile Organic Molecules in the Subsurface of the Atlantis Massif

Katherine A. Hickok
University of South Carolina

SERPENTINIZATION AND SYNTHESIS: SEARCHING FOR ABIOTIC AND BIOTIC NON-VOLATILE ORGANIC MOLECULES IN THE SUBSURFACE OF THE ATLANTIS MASSIF

by

Katherine A Hickok

Bachelor of Science
Clemson University, 2014

Submitted in Partial Fulfillment of the Requirements

For the Degree of Master of Science in

Geological Sciences

College of Arts and Sciences

University of South Carolina

2017

Accepted by:

Susan Lang, Director of Thesis

Lori Ziolkowski, Reader

Michael Bizimis, Reader

Cheryl L. Addy, Vice Provost and Dean of the Graduate School

ACKNOWLEDGEMENTS

Much appreciation must be given to the crews of the RSS James Cook, the operators of the RD2 and MeBO rock drills, and the ECORD and ESO operators. We truly appreciate the spectacular facilities of the Kochi Core Center and the assistance of Nan Xiao and the entire Geomicrobiology Group in processing samples. We would also like to thank the KCC for giving us the GX-P film and Escal Neo bags to analyze. We also like thank Mike Walla at the University of South Carolina Mass Spectrometry Services for the use of their GC-MS.

Funding for this research was provided by the U.S. Science Support Program Office subaward 23(GG00939-01) (NSF OCE-14-50528). Purchase of critical laboratory instrumentation was supported by awards from NSF-EAR/IF-1349539 and the Deep Carbon Observatory.

I would also like to personally thank my advisor, Susan Lang, for all of her support and assistance with this project, and for taking me to Japan. This degree was a once in a lifetime experience and I appreciate all of her guidance. Thanks again to my family, my old Clemson friends, and my new USC friends for helping and motivating me along the way.

ABSTRACT

High concentrations of hydrogen created during serpentinization can promote the formation of abiotic organic carbon molecules such as methane, formate, and short chain hydrocarbons and, in laboratory experiments, larger molecules containing up to 32 carbon atoms. Subsurface archaeal and bacterial communities can use these reduced compounds for metabolic energy. International Ocean Discovery Project Expedition 357 drilled 17 boreholes into the Atlantis Massif with the goals of investigating carbon cycling and the presence of life in a zone of active serpentinization. The expedition recovered multiple lithologies including gabbros, basalts, carbonate sands, and serpentinites. A subset of contrasting lithologies were analyzed for n-alkane and fatty acid content to determine if non-volatile organic molecules are produced abiotically in serpentinizing environments and to identify 'hot spots' of microbial life in the subsurface. Given the high potential for contamination during drilling, a suite of materials used in sample collection and processing were also analyzed to characterize their signatures.

Biologically-derived lipid biomarkers could not be identified in any of the samples, indicating any biological communities present in the subsurface of the

Massif were in abundances below our ability to detect them. An n-alkane series ranging from C_{18} to C_{30} with $\delta^{13}C$ isotopic values of -30.9‰ to -28.8‰ were present in various lithologically diverse samples. The distribution of these compounds was similar to those observed in previous grab samples from the same region, and to compounds formed abiotically in laboratory experiments. For the current set of samples, multiple lines of evidence point to the rock saw used to remove core exteriors during sample processing as the source of the n-alkanes. This result highlights the importance of careful prevention and characterization of contamination to allow for more accurate interpretations of complex and dynamic subsurface processes. Many of the other sample-handling procedures designed to reduce surface contamination were determined to be effective and should be implemented in future projects. The definitive detection and identification of abiotic and biological lipids in the subsurface of an actively serpentinizing system would be a significant step towards understanding the evolution of pre-biotic chemistry and life in extreme environments, but future reports of these compounds must occur in conjunction with thorough contamination assessments.

TABLE OF CONTENTS

ACKNOWLEDGEMENTS iii

ABSTRACT iv

LIST OF TABLES viii

LIST OF FIGURES ix

CHAPTER 1: INTRODUCTION 1

CHAPTER 2: BACKGROUND 7

CHAPTER 3: MATERIALS AND METHODS 13

3.1 SAMPLE COLLECTION AND PROCESSING 13

3.2 CONTAMINANT COLLECTION 15

3.3 SOLVENT EXTRACTION 16

3.4 GC-MS AND ISOTOPE ANALYSIS 17

CHAPTER 4: RESULTS 21

4.1 SAMPLE SELECTION CRITERIA 21

4.2 LIPIDS SIGNATURES OF POTENTIAL CONTAMINANTS 22

4.3 LIPID SIGNATURES OF SAMPLES 23

CHAPTER 5: DISCUSISON 32

5.1 STEPS TO MINIMIZE CONTAMINATION.....32

5.2 NO DEFINITIVE EVIDENCE FOR BIOTICALLY DERIVED LIPIDS ..34

5.3 SOURCE OF THE ALKANE SERIES 36

CHAPTER 6: CONCLUSIONS.....45

REFERENCES.....49

APPENDIX A: SUPPLEMENTAL INFORMATION 58

LIST OF TABLES

Table 3.1 Potential contaminants 19

Table 4.1 Samples selected for analyses 25

Table 4.2 N-alkane concentrations and $\delta^{13}C$ values.....26

Table 4.3 Fatty acid concentrations and $\delta^{13}C$ values 27

LIST OF FIGURES

Figure 2.1 Map of the Atlantis Massif 11

Figure 2.2 Key biotic and abiotic chromatograms 12

Figure 3.1 Sample processing steps 20

Figure 4.1 Core visualizations 28

Figure 4.2 H_2 and CH_4 fluid concentrations. 29

Figure 4.3 Rock saw and umbilical cord grease chromatograms 30

Figure 4.4 Expedition 357 sample chromatograms 31

Figure 5.1 $\delta^{13}C$ isotopic values compared to biologically derived lipids 43

Figure 5.2 $\delta^{13}C$ isotopic values compared to abiotically derived compounds 44

Figure A.1 Contaminant chromatograms: bags 58

Figure A.2 Contaminant chromatograms: gloves 59

Figure A.3 Contaminant chromatograms: oils 60

Figure A.4 Contaminant chromatograms: Shinfuji burner, RNase AWAY 61

Figure A.5 Expedition 357 chromatograms: cut serpentinites 62

Figure A.6 Expedition 357 chromatograms: cut samples 63

Figure A.7 Expedition 357 chromatograms: Milli-Q rinsed samples 64

CHAPTER 1

INTRODUCTION

Serpentinization is a series of spontaneous reactions that ensue when seawater hydrates olivine and pyroxene in ultramafic peridotites, ultimately producing serpentine, brucite, magnetite, and hydrogen (Moody, 1976). Environments where these reactions occur have the potential for the abiotic formation of organic molecules via Fischer-Tropsch Type (FTT) synthesis from the resulting hydrogen (Sherwood Lollar et al., 2002; Proskurowski et al., 2008). Volatile compounds such as methane, ethane, propane, butane, and formate have been identified in fluids from serpentinite-hosted hydrothermal systems and have been attributed to abiotic synthesis reactions (Kelley et al., 2001; 2005; Proskurowski et al., 2008; Lang et al., 2010). The steady production of these reduced compounds also provides a favorable habitat for chemolithotrophic and heterotrophic microbial communities (Schrenk et al., 2013). These environments may therefore represent a unique biome or provide insight in the physiochemical conditions needed to sustain life.

Serpentinization is widespread in the oceans and on continents. Seafloor spreading centers cause extension in the ultramafic- and mafic-dominated oceanic

lithosphere inducing detachment faulting, which uplifts these deep crustal and upper mantle rocks to form extensive massifs called oceanic core complexes (OCC) (Blackman et al., 2002; Früh-Green et al., 2004; Karson et al., 2006). Faulting-induced fractures promote seawater infiltration and circulation through subsurface peridotites resulting in the ideal conditions for serpentinization (Kelley et al., 2001; 2005; Früh-Green et al., 2003, Klein et al., 2015). Continental ophiolite complexes consist of emplaced oceanic mafic and ultramafic rocks that also undergo serpentinization processes (Barnes et al., 1967; 1978). The ubiquity of detachment faulting and fracturing along spreading centers implies that serpentinization processes are more widespread than have been currently recognized (Früh-Green et al., 2004) and suggests similar processes may have existed since early Earth (Sleep et al., 2011).

A major interest in serpentinizing systems is the potential for abiotic synthesis of organic molecules. Highly reducing environments thermodynamically favor abiotic organic compound formation catalyzed by iron- and nickel-bearing minerals (Shock and Schulte, 1998; Horita et al., 1999, Foustoukos and Seyfried, 2004). Laboratory experiments have demonstrated that long-chain non-volatile organic compounds containing up to 32 carbon atoms can be synthesized under serpentinizing conditions. (McCollom and Seewald, 2006). These types of aliphatic compounds are important since they could coalesce along

surfaces, such as the pore spaces in carbonate deposits, to form lipid bilayers that mimic cellular membranes (Martin and Russell, 2003). Phosphate- and boron-enriched minerals in similar locations can provide niches where these elements can be incorporated with abiotic organic compounds to synthesize nucleic acids (Holm et al., 2006; Ricardo et al., 2004). Verifying the presence of abiotically synthesized long-chain non-volatile organic molecules in field environments could provide strong evidence that similar processes could have played a central role in the formation of early life. As yet, none have been conclusively identified in field environments.

A second key interest in these environments is the ability of microbes to utilize the large quantities of metabolic energy generated from serpentinization reactions. The oxidation of the hydrogen produced during serpentinization fuels the metabolic activity of multiple archaeal and bacterial communities by acting as an electron donor (Kelley et al., 2005, McCollom, 2007a). Sulfur-, methane-, and hydrogen- cycling microorganisms have been identified in serpentinization environments throughout the world (Schrenk et al., 2004; 2013; Brazelton et al., 2006; Suzuki et al., 2013). However, most of these observations have been from surface settings where the presence of oxygen changes the types of microorganisms that can survive. The serpentinite subsurface comprises a large

geographical region that could support a significant and diverse microbial community, but direct observations of these ecosystems have yet to be made.

Recent research indicates similar reactions could be occurring on extraterrestrial bodies. Serpentinization reactions have been proposed to occur on Mars (Oze and Sharma, 2005), Enceladus (Malamud and Prialnik, 2013), and Titan (Niemann et al., 2005, Tobie et al., 2006). Spectral signatures of aliphatic organic molecules were identified on the surface of the dwarf planet Ceres, localized in a region of ammonium-bearing hydrated phyllosilicates, carbonates, and water ice (De Sanctis et al., 2017). While the mechanism for how these compounds were generated is unknown, it is speculated that aqueous hydrothermal alteration on Ceres could be the source (De Sanctis et al., 2015; De Sanctis et al., 2016; Ammannito et al., 2016; Combe et al., 2016). Certain phyllosilicate minerals are serpentinization products (Nozaka et al., 2008) that are capable of adsorbing organic compounds onto their surfaces (Pearson et al., 2002; Hedges et al., 1977). Thus, if organic compounds are present, they could be localized in regions of active serpentinization. Ironically, it may be easier to identify abiotically produced organic molecules on extraterrestrial bodies where the organic signatures of life do not interfere with the abiogenic signals.

To date, biological lipids have been identified in serpentinites from the Atlantis Massif and the Iberia Margin (Delacour et al., 2008; Klein et al., 2015).

Multiple isoprenoidal biomarkers and an n-alkane series were discovered in the Atlantis Massif samples (Delacour et al., 2008). Bacterial nonisoprenoidal dialkylglycerol diether (DEG) lipids, archeaol, and acyclic glycerol dibiphytanyl glycerol tetraether (GDGT) lipids were identified in brucite-calcite veins from Iberia Margin serpentinites (Klein et al., 2015). However, samples from both locations were surface exposed and may not be representative of in situ processes. The Atlantis Massif samples were collected via submersible from the seafloor (Delacour et al., 2008), while the Iberia Margin samples were originally drilled in 1993 and stored in a non-sterile fashion in an oxygenated atmosphere before being subsampled in 2014 (Klein et al., 2015). Previous subsurface samples collected from the Atlantis Massif did not include serpentinites. Thus, pristine subsurface serpentinites have not yet been examined for biological or abiotic lipids.

Due to the inherently low abundances of biomass and other organic compounds suspected to be present in the subsurface, it is essential to prevent contamination during sample collection and of the collected rock cores. Cell counts are anticipated to be low, and similar compounds could be present in the multiple oils, greases, and plastics used during drilling and handling processes (Yanagawa et al., 2013). Therefore, it is critical to implement contaminant testing to indicate if collected samples were compromised and could affect the geochemical and microbiological analyses.

The goals of this research are to investigate biotic and abiotic synthesis reactions that occur in serpentinizing environments present in subsurface rocks. Specifically, we seek 1) to determine if long-chain, non-volatile abiotic organic molecules are present in the oceanic serpentinite subsurface and 2) to determine if biological lipids can be identified and, if so, identify what types of lithologies and physicochemical regimes they are associated with.

CHAPTER 2

BACKGROUND

The recent discovery of the low-temperature Lost City Hydrothermal Field upon the Atlantis Massif (Figure 2.1), located off-axis of the Mid-Atlantic ridge, provides an excellent opportunity to understand how active serpentinization influences the oceanic subsurface biosphere and carbon cycle (Kelley et al., 2001). Thus, it has been the target of multiple International Ocean Discovery Program expeditions. The recently completed Expedition 357 drilled 17 boreholes across the massif "to explore the subsurface environment, the potential for a hydrogen-based deep biosphere, and hydrocarbon synthesis in an active serpentinite-hosted hydrothermal system" (Früh-Green et al., 2010).

The Atlantis Massif is an OCC uplifted between 1.5 and 2 million years ago at the intersection of the Mid-Atlantic Ridge and the Atlantis Transform Fault (Karson et al., 2006; Früh-Green et al., 2004; Kelley et al., 2001). The Lost City Hydrothermal Field (LCHF) lies at the peridotite-dominated southern end, which is one of the most studied regions of active serpentinization in the ocean (Kelley et al., 2001). Throughout the 400 m length field, there are multiple 60 m high carbonate-brucite chimneys that, for the past 30,000 to >100,000 years, have been

venting reducing fluids that are both warm (41-90°C) and alkaline (9-11) (Kelley et al., 2001, 2005; Früh-Green et al., 2003; Ludwig et al., 2011). These hydrothermal fluids contain elevated concentrations of hydrogen (1-15 mmol/kg), methane (1-2 mM), short-chain alkanes (C_2-C_4) (1-2 nmol/kg), and formate (36-146 μM) (Kelley et al., 2001; 2005; Proskurowski et al., 2008; Lang et al., 2010). The alkaline, Ca^{2+}-rich hydrothermal fluids react with any available CO_2 or dissolved inorganic carbon (DIC), rapidly precipitating calcium carbonate ($CaCO_3$). This process can happen in the subsurface during seawater downwelling (Eickmann et al., 2009a, Proskurowksi et al., 2008), with mantle-derived CO_2, (Eickmann et al., 2009b), and after fluids exit the seafloor and mix with deep ocean water (Kelley et al., 2001; 2005; Ludwig et al., 2006; Greene et al., 2015). Fluids at Lost City and continental serpentinite-hosted springs therefore contain vanishingly small amounts of dissolved inorganic carbon (Bradley et al., 2009; Schrenk et al., 2010; Schwarzenbach et al., 2013). Sulfate is present in milli-molar concentrations in the Lost City fluids and is the dominant sulfur phase in the basement peridotites (Kelley et al., 2005; Delacour et al., 2008; Lang et al., 2012).

The chimney structures of the Lost City Hydrothermal field, located adjacent to the drill locations of Expedition 357, harbor biofilms that help precipitate calcium carbonate and have been the focus of many microbiological and geochemical studies. (Kelley et al., 2001; Schrenk et al., 2004; Bradley et al.

2009; Brazelton et al., 2011; Lang et al., 2012; Méhay et al., 2013). These biofilms are dominated by a methane-cycling archaea known as the Lost City Methanosarcinales (Schrenk et al., 2004; Brazleton et al., 2006). Additionally, geochemical trends across the field strongly indicate that microbial sulfate reduction is occurring in the subsurface (Proskurowski et al., 2006; Lang et al., 2012). Given these microbiological and geochemical studies of the LCHF, methane-cycling archaea and sulfate reducing bacteria are the most likely organisms to be present in the Atlantis Massif subsurface (Schrenk et al., 2004; Brazelton et al., 2006).

Previous organic geochemical analysis of rocks collected from the Atlantis Massif identified organic molecules in surficial and subsurface serpentinites and gabbros (Delacour et al., 2008). Surficial rocks collected by submersible from the southern wall and subsurface rocks drilled from the central dome IDOP Site 1309D contained a saturated hydrocarbon distribution of long-chain n-alkanes and isoprenoidal compounds including phytane, pristane, norpristane, and squalane (Figure 2.2a, Delacour et al., 2008). Carbon isotopic analyses on the surface grab samples had $\delta^{13}C$ values ranging from -38.6‰ to -24.6‰ (Delacour et al., 2008). The rocks recovered by drilling did not contain enough material for isotope analyses and no serpentinites were recovered (Delacour et al., 2008). These compounds were interpreted to be from marine dissolved organic carbon (DOC)

incorporated during seawater circulation through the massif and subsequent sorption onto serpentinized phyllosilicate minerals (Delacour et al., 2008). The possibility that FTT synthesis could have generated some of these compounds could not be ruled out, but the lack of isotopic data from the central dome samples along with the presence of isoprenoids and higher n-alkane abundances suggests that, instead, marine DOC was the source of the compounds present in these specific samples (Delacour et al., 2008).

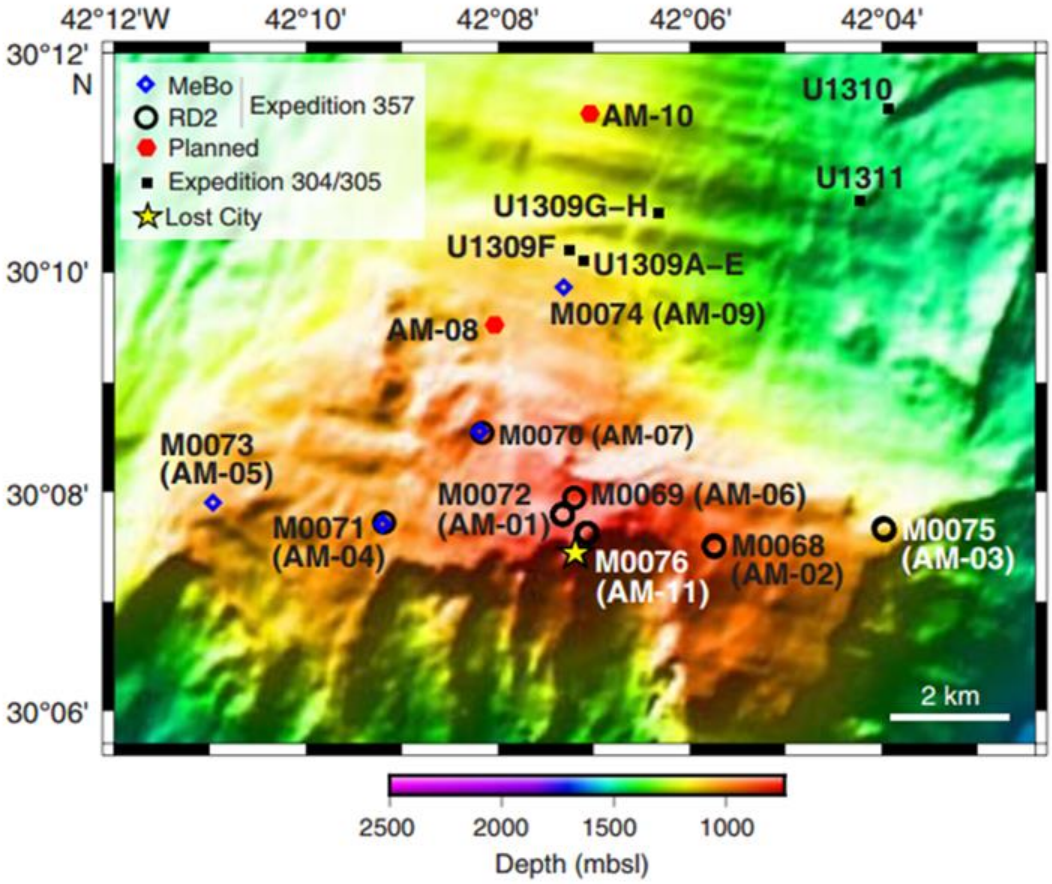

Figure 2.1 Map of the Atlantis Massif. Locations of RD2 (black circle) and MeBo (blue diamond) cored sites overlain on multibeam bathymetry (50m resolution) acquired during Expedition 357. Yellow star pinpoints the Lost City hydrothermal field, while the black square denotes locations of cored sites from Expedition from 304/305 and planned Expedition 357 sites (red circle) that were not drilled. Figure reproduced from Früh-Green et al., 2017a.

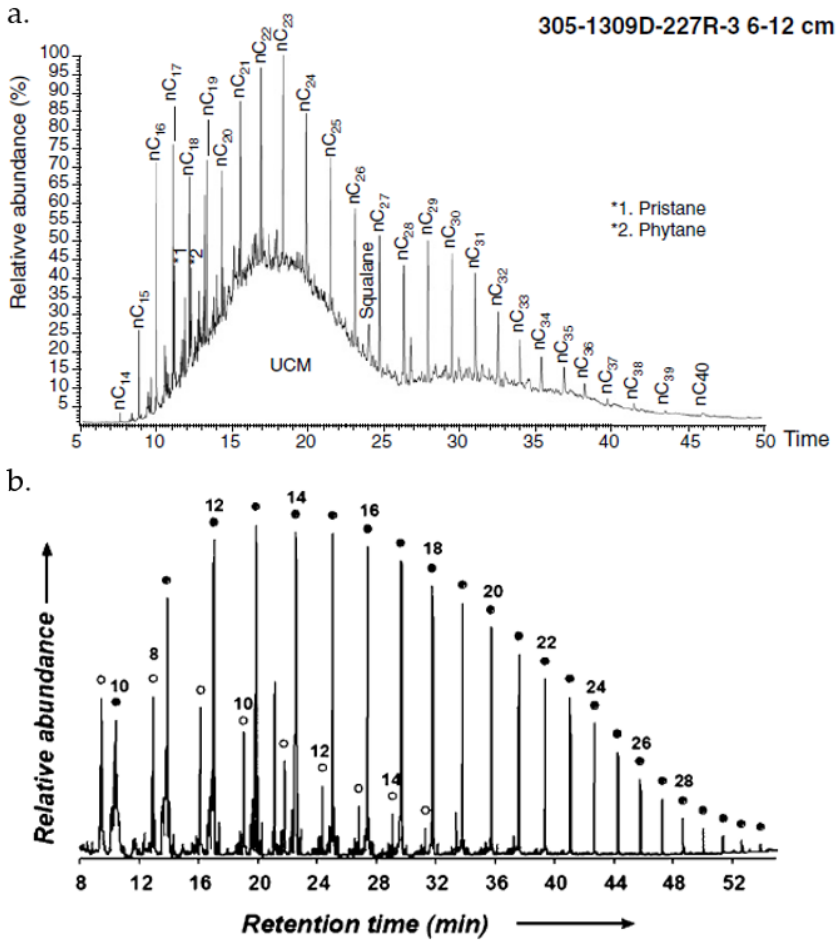

Figure 2.2 Key biotic and abiotic chromatograms. GC/MS chromatograms displaying the distribution of n-alkanes, isoprenoids, and alcohols from both biotic sources in Atlantis Massif samples (a.) and abiotic FTT synthesis experiments (b.). Reproduced from Delacour et al., 2008 (a.) and McCollom and Seewald, 2007b (b.).

CHAPTER 3

MATERIALS AND METHODS

3.1 Sample collection and processing

Rock samples analyzed in this study were collected during IODP Expedition 357 which drilled a North-South and an East-West profile of continuous core sequences across the Atlantis Massif (Figure 2.1), specifically targeting sites that are anticipated to be dominated by active serpentinization, microbial activity, and fluid flow (Früh-Green et al., 2017a). Two sea-bed rock drills, the MARUM Center for Marine Environmental Sciences Meeresboden-Bohrgerät 70 (MeBo) and the British Geological Survey RockDrill2 (RD2), recovered approximately 50 m of core with multiple lithologies including serpentinites, carbonate sands, basalts, and gabbros (Früh-Green et al., 2017a).

Upon arrival on deck, a small whole-round core (WRC) was cut and processed immediately for time-sensitive microbiological and geochemical analysis (Figure 3.1). Approximately half of these samples were flame-sterilized to eliminate surficial microbial contamination while the remainder were not flame sterilized. In both cases, the WRC was then wrapped in acid-washed and autoclaved Teflon sheeting and placed in gas tight Escal Neo bags that were

flushed with N_2 and heat sealed to maintain anoxic conditions. The bags were then frozen at -80°C for shore-based processing at the Kochi Core Center.

At the Kochi Core Center, the frozen WRCs were further processed, homogenized, and distributed. These activities took place within a class 10,000 clean room to minimize the contribution of cells and particles through air transfer (Masui et al., 2009). If the rock cores were large enough, the exterior was removed using a specialized diamond-tipped rock saw that had a chilled cooling plate. This design eliminated the need for cooling water and thus minimized the introduction of microbial or organic surficial contaminants. The rock saw isolated within a clean booth under HEPA-filter units (Masui et al., 2009). All rock saw surfaces, including the entirety of the band saw blade, were cleaned with RNase AWAY and methanol between each sample. If the rock cores were too small for cutting or composed of rubble, they were placed into combusted (5 hr, 500°) glass beakers and rinsed 10 times with Milli-Q water. After being cut or rinsed, the samples were crushed and homogenized with stainless steel impact mortars and pestles into a fine powder, which were cleaned with RNase AWAY and methanol between each sample to prevent cross contamination. Homogenization with impact mortars was performed while working between a KOACH benchtop laminar flow system. Due to time constraints at the Kochi Core Center, eleven samples were processed at Bigelow Laboratory for Ocean Sciences. The same homogenized powders were

distributed to multiple principal investigators so that samples would be subjected to multiple geochemical and microbiological analyses.

3.2 Contaminant collection

Sixteen samples of potential contaminants were collected before, during, and after the expedition (Table 3.1). They included laboratory gloves that were available for use on the ship, at the Kochi Core Center, and in-house: Semperguard Xpert, VWR Nitrile 112-2373, VWR Nitrile 112-2371, and KC500 purple nitrile gloves (VWR 32934-082). Four different bags and plastics were tested to determine their suitability for sample storage: Escal Neo, GX-P film, nylon sheeting (VWR P/N 12243-186), and Teflon sheeting (McMaster Carr P/N 8569K75, 36" wide x 0.003" thickness x 20' length). The Escal Neo, GX-P film, and nylon sheeting were rinsed with 9:1 DCM:MeOH before testing. The Teflon sheeting was acid washed with a 10% HCl soak overnight, then Milli-Q soak overnight. Five types of oils and greases used to operate rock drills and the ship were tested: MeBo transformer oil, B30 transformer oil, Atlantis hydraulic oil, MeBo hydraulic oil, and umbilical cord grease. RNase AWAY and a Shinfuji burner were used to remove ribonuclease contamination and to flame-sterilize samples, respectively. To collect potential contaminants from the rock saw, combusted filters dipped in methanol were wiped along the diamond-tipped blade and plate after the rock saw was cleaned

in the typical fashion then the blade was run for 1 minute. This focused on areas where the WRC was in contact with the saw during the exterior removal process.

3.3 Solvent extraction

Prior to extraction, 19 rocks and sands were freeze-dried to remove water. Each rock sample was ultrasonically extracted three times with methanol (MeOH), three times in a 3:1 mixture of dichloromethane (DCM): MeOH, and two times with DCM. Multiple samples of freshly combusted (5 hrs, 500°C) sand were treated identically to assess any contamination introduced during extraction and processing. Gloves and bags were cut into 2 gram pieces then ultrasonically extracted three times with 9:1 DCM:MeOH. A small aliquot of the grease samples were also extracted three times with 9:1 DCM:MeOH. The oil samples were tested by dissolving 10 μL of oil into 1 mL of hexane.

Extracts were combined and concentrated by rotary evaporation. If needed, samples were filtered through combusted glass wool to remove particles. The filtered solvent was then passed through a column of Na_2SO_4 to remove water. The remaining total lipid extract was separated over a Sepra™ NH_2 (Sigma-Aldrich P/N 57212-U) bulk packing column into multiple fractions by eluting with solvents of increasing polarity: F1: n-alkanes (eluted with hexane), F2: esters and ketones (eluted with 3:1 hexane: DCM), F3: alcohols and sterols (eluted with 9:1 DCM:

acetone), and F4: fatty acids (eluted with 4% formic acid in DCM). Elemental sulfur was removed from the n-alkane (F1) fraction using activated copper. The fatty acid (F4) fraction was methylated with HCl/MeOH (8% w/v) at 45˚C for 14 hours. These fractions were dissolved in a known volume of hexane prior to gas chromatography- mass spectrometry (GC-MS) and gas chromatography-combustion- isotope ratio mass spectrometry (GC-C-IRMS) analyses.

3.4 GC-MS and isotope analysis

The n-alkane and fatty acid fractions were analyzed by GC-MS on an Agilent Technologies 5975 Inert XL Mass Selective Detector with an Agilent J&W GC HP-5MS UI capillary column capillary column (30 m × 0.25 mm; 0.25 μm film thickness) using He as a carrier gas. Samples were injected in pulsed splitless mode. The temperature program was 70-150 ˚C (15 ˚C/min), 150-200 ˚C (5 ˚C/min), 200-300 ˚C (5 ˚C/min), and held at 300 ˚C for 10 minutes. Concentrations of each peak were quantified by comparison to a four- point standard curve of either a C_{7}-C_{30} alkane series (P/N 49451-U, Sigma Aldrich) or a mixture of 37 fatty acids (P/N 47885-U, Sigma Aldrich).

The compound-specific carbon isotope ratios for each n-alkane and fatty acid fraction were analyzed by GC-C-IRMS using a Thermo Trace 1310 gas chromatograph with a Thermo GC IsoLink II with an Agilent DB-5 capillary

column (30 m × 0.25 mm, 0.25 μm film thickness) with helium as the carrier gas. A Gerstel CIS-6 inlet was held in splitless mode during injection then set to a 10:1 split after three minutes. The column inlet temperature program was initially at 40 ˚C then ramped to 150 ˚C at 16 ˚C/min, and then ramped to 300 ˚C at 12 ˚C/min. The temperature program of the GC was initially held at 45 ˚C for one minute then ramped to 130 ˚C at 40 ˚C/min, then ramped to 250 ˚C at 6 ˚C/min, then ramped to 290 ˚C at 2 ˚C/min, then ramped to 320 ˚C at 6 ˚C/min, and then held at 320 ˚C for six minutes. Each sample was injected in duplicate and a standard mixture of n-alkanes (A6 Standard, Arndt Schimmellman, Indiana University) with known isotopic composition was analyzed every third injection as an external isotope standard and to monitor system performance. The isotopic signatures of the fatty acids were corrected for the contribution of additional carbon during methylation. The standard deviation of duplicate injections ranged from 0.00 to 0.43. The carbon isotope ($\delta^{13}C$) ratios of each compound are expressed as per mil (‰) relative to the Vienna Pee Dee Belemnite (VPDB).

Table 3.1 Potential contaminants. List of potential contaminants and their uses.

Name	Description and use
Umbilical cord grease	Grease used to lubricate umbilical cord that remotely powered and controlled the RD2 rock drill
B30 transformer oil	Highly refined hydrotreated light naphthenic oil used to insulate, suppress corona and arcing, and to serve as a coolant for transformers
MeBo transformer oil	Oil used to insulate, suppress corona and arcing, and to serve as a coolant for the transformers of the MeBo rock drill
MeBo hydraulic oil	Oil used to transfer power in hydraulic machinery on the MeBo rock drill
Atlantis 22 hydraulic oil	Bio-hydraulic oil based on saturated synthetic esters used to transfer power in hydraulic machinery, used on RD2 rock drill
RNase AWAY	Solution used to remove ribonuclease contamination from plastics, glassware, and the chilled rock saw to prevent RNA degradation
Shinfuji burner	Blowtorch used to flame sterilize samples, mortars, and pestles
Acid-washed PTFE Teflon	Acid washed teflon used to wrap samples before being place in Whirlpak bags
Nylon	Plastic used in clean rooms; tested but not used
GX-P film	Potential bag that could have been used for sample storage that maintains anaerobic conditions
Escal Neo bag	Potential bag that could have been used for sample storage that maintains anaerobic conditions
Semperguard Xpert gloves	Gloves used when handling and processing samples on the ship and at the Kochi Core Center
VWR P/N 112-2371 gloves	Gloves tested but not used for sample handling
VWR P/N 112-2373 gloves	Gloves tested but not used for sample handling
KC500 purple nitrile gloves	Gloves used when handling and processing samples during in house procedures
Rock saw	Specialized diamond-tipped rock saw that had a chilled cooling plate at the KCC used to remove exteriors from WRC

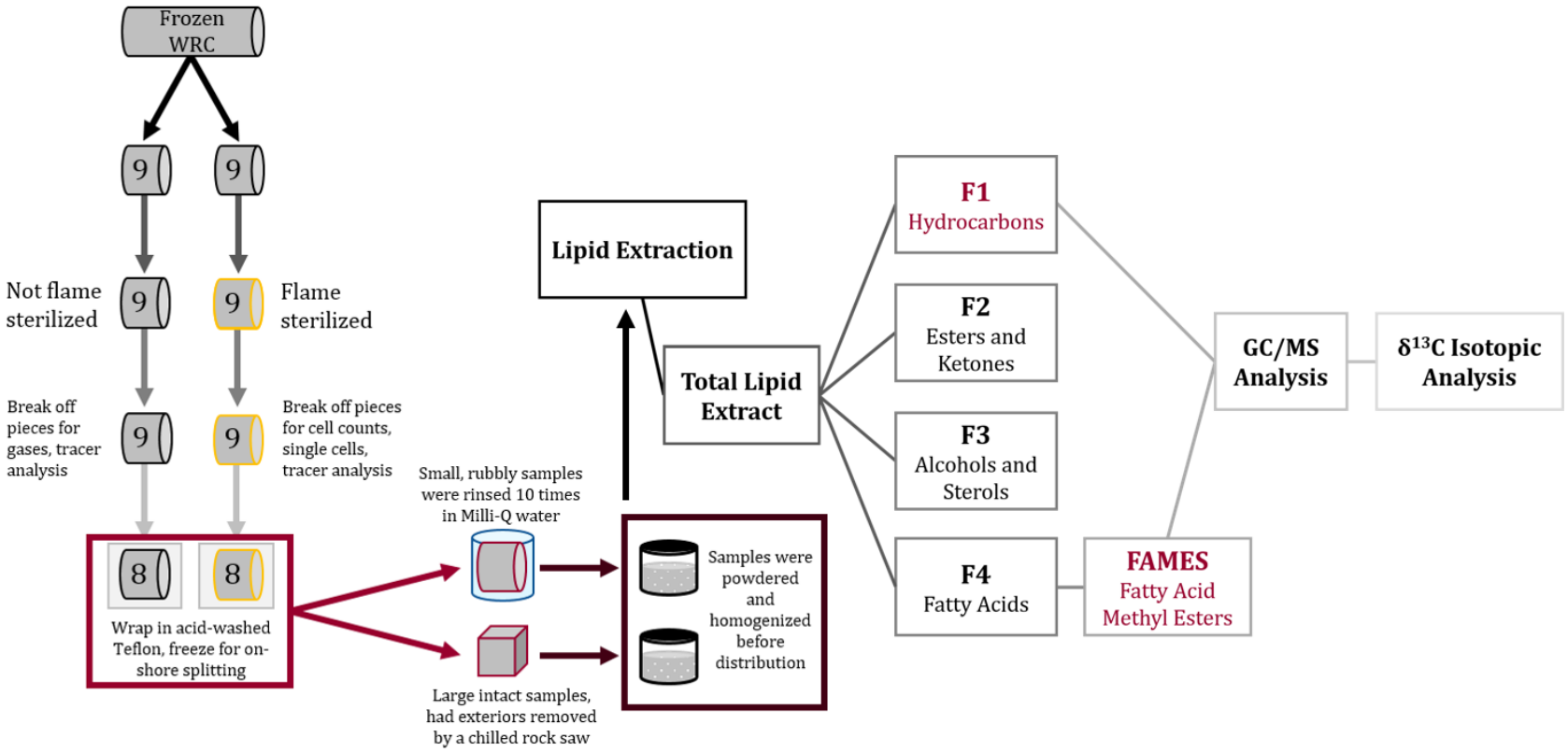

Figure 3.1 Sample processing steps. Schematic of core handling, sample processing, and lipid extraction procedures used offshore, at the Kochi Core Center, and during in-house extraction and separation procedures.

CHAPTER 4

RESULTS

4.1 Sample selection criteria

Of the 60 core samples obtained from 17 boreholes during the expedition, 19 rocks and sands were carefully selected because they were expected to represent drill sites with the greatest probability of finding lipid biomarkers (Table 4.1, Figure 4.1). Initial efforts were focused on sites 69, 72, and 76 which are located on the central dome of the Atlantis Massif and are closest to the Lost City Hydrothermal Field. Shipboard gas analysis of subsurface fluids exiting these drilled boreholes indicated that these central dome sites contain the highest H_2 and CH_4 concentrations (Figure 4.2, Früh-Green et al., 2017b) and are therefore likely to be zones of active serpentinization. Preference was also given to samples that had high volumes and had the exterior removed by cutting rather than Milli-Q rinsing. These specimens were expected to be more representative of in situ conditions and be exposed to less contamination than those that have been rinsed with Milli-Q water. To determine if there were lithological relationships with the presence of biomarkers, samples from a variety of rock types (serpentinites, gabbros, basalts, and carbonate sands) were also selected.

4.2 Lipid signatures of potential contaminants

The saturated hydrocarbon chromatograms for the potential contaminant samples varied highly. The Escal Neo bag and GX-P film chromatograms contained a series of even-numbered alkanes ranging from C_{14} to C_{30}, but lacked bell-shaped humps, also known as unresolved complex mixtures (UCM), caused by the coelution of many cyclic and branched compounds that the gas chromatograph cannot fully resolve (Figure A.1). The nylon and Teflon sheeting chromatograms were relatively clean and had an absence of peaks (Figure A.1). The hydrocarbon fraction of the four glove types used during sample processing and handling showed large UCMs with the two VWR gloves containing elevated concentrations of benzene hydrocarbons and the KC500 gloves containing the same compounds as above plus an identifiable n-alkane series ranging from C_{22} to C_{27} (Figure A.2).

The hydrocarbon fraction of the four transformer and hydraulic oils used during drilling were dominated by UCMs (Figure A.3). The umbilical cord grease chromatogram was comprised of a series of alkanes ranging from C_{16} to C_{32} with an average isotopic signature of -31.2 ± 0.3‰ and a slight even-over-odd carbon number predominance (Figure 4.3). The Shinfuji burner, used to sterilize samples, and the RNase AWAY solution, used to remove ribonuclease contamination, chromatograms contained no observable UCM except for the a high abundance of

phthalates in the Shinfuji burner chromatogram (Figure A.4). The rock saw chromatogram contained a series of n-alkanes ranging from C_{18} to C_{32} with no odd over even carbon number predominance (Figure 4.3). Compound-specific isotope analysis of these compounds range from -31.0‰ to -30.1‰ with an average value of -30.6 ± 0.4‰.

Thirteen contaminants contained hexadecanoic acid and nine contaminants contained octadecanoic acids in their fatty acid chromatograms. The compound specific $\delta^{13}C$ isotopic analysis of the fatty acids exhibited a large range, between -30.9‰ and -25.2‰ for C_{16} fatty acids and between -30.4‰ and -24.8‰ for C_{18} fatty acids.

4.3 Lipid signatures of samples

The saturated hydrocarbon fraction of extracted core samples contained either a characteristic series of n-alkanes ranging from C_{18} to C_{30} and up to C_{32} or contained no detectable n-alkanes (Figures 4.4, A.5, A.6). Concentrations of measurable saturated hydrocarbons ranged from 6- 180 ng/g rock (Table 4.2). Of the 11 samples that contained the n-alkane series, there was no relationship with lithology or amount of sample extracted. The highest n-alkane concentrations occurred in carbonate sand and lithics 69A 4R1 U 121-131 and serpentinite 76B 9R1 F 34-41, and the lowest concentrations occurred in gabbro 71A 2R1 F 67-77 and

serpentinite 76B 10R1 U 91-111. The chromatogram of the n-alkane series showed no odd or even carbon number predominance, and abundances decreased as carbon number increases (Figures 4.4, A.5, A.6).

Compound-specific isotope analysis of the saturated hydrocarbons ranged from -30.9‰ to -28.8‰ with an average value of -30.3 ± 0.4‰ for samples that contained enough material for isotopic analysis (Table 4.2). The isotopic values were uniform between n-alkane and lithology.

The fatty acid fraction of extracted samples contained predominantly hexadecanoic (6- 159 ng compound/ g rock) and octadecanoic (10- 1200 ng compound/ g rock) fatty acids (Table 4.3). All samples contained detectable C_{18} fatty acid and all but five samples contained C_{16} fatty acid. Carbonate sands 69A 4R1 U 75-85 and 74A 1R1 U 10-20 contained approximately 10-100 times higher concentrations of octadecanoic acid (535 and 1200 ng compound/ g rock, respectively) than the remaining samples. Compound-specific $\delta^{13}C$ isotope analysis of octadecanoic acids ranged from -28.3‰ and -31.9‰ with an average of -29.9 ± 1.0‰ (Table 4.3). The only sample with sufficient hexadecanoic acid for isotope analysis had a $\delta^{13}C$ value of -29.8‰. The isotopic values for the C_{18} fatty acids did not vary between lithology and no other trends were apparent.

Table 4.1 Samples selected for analyses. List of samples selected for extraction with detailed descriptions summarized from Onshore Section Overview Reports, how each sample was processed, and amount processed.

Expedition/ Hole	Sample name	Depth (mbsf)	Generalized lithology	Detailed description	Sample processing
357-69A	4R1 U 75-85 cm	5.91	Carbonate sand	Pelagic carbonate ooze with fine grained lithic fragments including basaltic fragments up to 4 mm in size	Interior sampled with syringe
357-69A	4R1 U 121-131 cm	6.37	Carbonate sand and lithics	Pelagic carbonate ooze with fine grained lithic fragments including basaltic fragments up to 4 mm in size with rubbly angular fragments of mostly serpentinized harzburgite	Exterior removed by chilled rock saw and rinsed 10 times in Milli-Q water
357-69A	5R1 F? 137-151 cm	8.25	Gabbro	Metadolerite with light toned alteration patched determine by XRD to be chlorite with abundant epidote veins	Exterior removed by chilled rock saw
357-69A	10R1 F 104-124 cm	15.76	Serpentinite	Serpentinized pyroxene-rich harzburgite which is cut by a carbonate vein	Exterior removed by chilled rock saw
357-70A	2R1 U 87-97 cm	2.65	Basalt	Carbonate-cemented basaltic breccia with both a reddish oxidized and light cream colored carbonate matrix	Exterior removed by chilled rock saw
357-70A	3R1 F 19-29 cm	3.05	Basalt	Sparsely vesicular basalt breccia in a carbonate matrix; orange sediment contains glassy fragments	Exterior removed by chilled rock saw
357-70A	3R1 U 29-38 cm	3.15	Basalt	Sparsely vesicular basalt breccia in a carbonate matrix; orange sediment contains glassy fragments	Rinsed 10 times in Milli-Q water (Bigelow)
357-71A	1R2 F 0-11 cm	0.58	Serpentinite	Serpentinized dunite with “disseminated” trains of spinels and numerous carbonate veins; serpentinization is complete with oxidation concentrated close to carbonate veins	Exterior removed by chilled rock saw
357-71A	2R1 F 67-77 cm	3.39	Gabbro	Metagabbro with clear leucocratic domains (likely troctolitic)	Exterior removed by chilled rock saw
357-71B	3R1 U 0-10 cm	3.44	Serpentinite	Rubble of serpentinized harzburgite with metagabbro interval	Rinsed 10 times in Milli-Q water
357-71C	3R1 U 0-2,4-10 cm	5.02	Serpentinite	Angular to rounded fragments of serpentinised harzburgite up to 4cm in size. Some fragments partly oxidized	Rinsed 10 times in Milli-Q water
357-72B	5R1 U 40-43 cm	6.39	Schist	Talc-amphibole-chlorite schist with a strong foliation and a lineation can be seen on the foliation surface with boudinaged dolerite fragments and rare sulfides and oxides	Rinsed 10 times in Milli-Q water
357-72B	8RCC F 5-20 cm	12.33	Serpentinite	Serpentinized porphyroclastic harzburgite with late serpentinized veins; cataclasis through several vein events with irregular whitish veins, branching, showing schistosity	Exterior removed by chilled rock saw
357-74A	1R1 U 10-20 cm	0.1	Carbonate sand	Fossiliferous carbonate sand with abundant foraminifera, rare lithic fragments of basalt to 5 mm	Interior sampled with syringe
357-76B	5R1 U 14-28 cm	6.87	Serpentinite	Serpentinized dunite with high degree of serpentinization; partially sheared mesh texture; strong pervasive oxidation; fracture network exploited by irregular veins	Exterior removed by chilled rock saw
357-76B	5R1 F 28-36 cm	7.01	Serpentinite	Serpentinized dunite with high degree of serpentinization; partially sheared mesh texture; strong pervasive oxidation; fracture network exploited by irregular veins	Rinsed 10 times in Milli-Q water (Bigelow)
357-76B	9R1 F 34-41 cm	13.21	Serpentinite	Highly oxidized porphyroclastic serpentinized harzburgite with pockets of talc-rich material and oxidized calcite veins; highly cataclastic and fractured structure with no deformation	Exterior removed by chilled rock saw
357-76B	9R1 U 43-52 cm	13.3	Serpentinite	Highly oxidized porphyroclastic serpentinized harzburgite with pockets of talc-rich material and oxidized calcite veins; highly cataclastic and fractured structure with no deformation	Exterior removed by chilled rock saw
357-76B	10R1 U 91-111 cm	15.5	Serpentinite	Fractured serpentinized dunite breaking down into fragments	Exterior removed by chilled rock saw

Table 4.2 N-alkane concentrations and $\delta^{13}C$ values. Concentrations and $\delta^{13}C$ compound-specific isotopic signatures of n-alkanes extracted from the Atlantis Massif subsurface.

Sample name	69A 4R1 U 121-131		69A 5R1 F? 137-151		69A 10R1 F 104-124		70A 2R1 U 87-97		70A 3R1 F 19-29		71A 1R2 F 0-11		71A 2R1 F 67-77		76B 5R1 U 14-28		76B 9R1 F 34-41		76B 9R1 U 43-52		76B 10R1 U 91-111	
Amount (g)	20.35		30.78		43.93		68.48		31.52		48.7		88.41		41.3		20.3		17.02		67.75	
	ng compound/ g rock	$\delta^{13}C$ (‰)	ng compound/ g rock	$\delta^{13}C$ (‰)	ng compound/ g rock	$\delta^{13}C$ (‰)	ng compound/ g rock	$\delta^{13}C$ (‰)	ng compound/ g rock	$\delta^{13}C$ (‰)	ng compound/ g rock	$\delta^{13}C$ (‰)	ng compound/ g rock	$\delta^{13}C$ (‰)	ng compound/ g rock	$\delta^{13}C$ (‰)	ng compound/ g rock	$\delta^{13}C$ (‰)	ng compound/ g rock	$\delta^{13}C$ (‰)	ng compound/ g rock	$\delta^{13}C$ (‰)
Alkanes																						
C_{18}	21	b.d.l.	-	-	-	-	6	b.d.l.	-	-	-	-	-	-	14	b.d.l.	-	-	-	-	-	-
C_{19}	22	b.d.l.	-	-	-	-	7	b.d.l.	-	-	-	-	-	-	15	b.d.l.	21	b.d.l.	-	-	-	-
C_{20}	30	b.d.l.	-	-	-	-	7	b.d.l.	-	-	-	-	-	-	16	b.d.l.	36	-30.2	-	-	-	-
C_{21}	48	-30.4	14	b.d.l.	-	-	10	b.d.l.	13	b.d.l.	20	b.d.l.	-	-	24	-30.4	68	-30.7	32	b.d.l.	-	-
C_{22}	86	-30.7	16	b.d.l.	10	b.d.l.	16	-30.3	13	b.d.l.	21	b.d.l.	-	-	34	-30.4	104	-30.6	43	-30.6	-	-
C_{23}	104	-30.4	17	b.d.l.	11	b.d.l.	20	-30.3	14	b.d.l.	21	b.d.l.	5	b.d.l.	41	-30.5	139	-30.7	47	-30.4	7	b.d.l.
C_{24}	113	-30.6	17	b.d.l.	12	b.d.l.	22	-30.2	15	b.d.l.	22	b.d.l.	5	b.d.l.	44	-30.3	139	-30.8	45	-30.2	7	b.d.l.
C_{25}	103	-30.3	19	b.d.l.	14	-30.2	22	-30.2	15	b.d.l.	22	b.d.l.	6	b.d.l.	44	-30.3	180	-30.8	45	b.d.l.	9	b.d.l.
C_{26}	96	-30.6	19	b.d.l.	14	-30.0	20	-30.4	15	b.d.l.	22	b.d.l.	6	b.d.l.	42	-30.4	154	-30.7	42	b.d.l.	9	b.d.l.
C_{27}	81	-30.3	17	b.d.l.	coelute	-29.2	18	-30.3	12	b.d.l.	21	b.d.l.	6	b.d.l.	38	-30.1	130	-30.7	37	b.d.l.	9	b.d.l.
C_{28}	75	-30.7	19	b.d.l.	15	-28.8	16	-30.3	13	b.d.l.	22	b.d.l.	-	-	37	-30.6	113	-30.9	39	b.d.l.	9	b.d.l.
C_{29}	55	-30.5	19		15	b.d.l.	15	-30.3	13	b.d.l.	21	b.d.l.	-	-	34	-30.5	97	-30.7	39	b.d.l.	9	b.d.l.
C_{30}	60	b.d.l.	-	-	14	b.d.l.	12	b.d.l.	13	b.d.l.	-	-	-	-	32	-30.7	82	-30.6	-	-	9	b.d.l.

Table 4.3 Fatty acid concentrations and $\delta^{13}C$ values. Concentrations and $\delta^{13}C$ values of fatty acid methyl esters extracted from the Atlantis Massif subsurface.

Expedition/ Hole	Sample name	hexadecanoic acid, ME		octadecanoic acid, ME	
		ng compound/ g rock	$\delta^{13}C$ (‰)	ng compound/ g rock	$\delta^{13}C$ (‰)
357-69A	4R1 U 75-85 cm	141	b.d.l.	535	-29.8
357-69A	4R1 U 121-131 cm	11	b.d.l.	47	b.d.l.
357-69A	5R1 F? 137-151 cm	18	b.d.l.	59	-28.3
357-69A	10R1 F 104-124 cm	6	b.d.l.	coelute	b.d.l.
357-70A	2R1 U 87-97 cm	7	b.d.l.	63	-29.2
357-70A	3R1 F 19-29 cm	7	b.d.l.	32	b.d.l.
357-70A	3R1 U 29-38 cm	31	b.d.l.	75	-30.2
357-71A	1R2 F 0-11 cm	-	-	10	b.d.l.
357-71A	2R1 F 67-77 cm	-	-	27	b.d.l.
357-71B	3R1 U 0-10 cm	12	b.d.l.	coelute	-31.9
357-71C	3R1 U 0-2,4-10 cm	87	b.d.l.	132	b.d.l.
357-72B	5R1 U 40-43 cm	52	b.d.l.	141	-30.8
357-72B	8RCC F 5-20 cm	28	-29.8	156	-30.2
357-74A	1R1 U 10-20 cm	159	b.d.l.	1200	-29.1
357-76B	5R1 U 14-28 cm	-	-	114	-29.9
357-76B	5R1 F 28-36 cm	-	-	125	b.d.l.
357-76B	9R1 F 34-41 cm	21	b.d.l.	39	b.d.l.
357-76B	9R1 U 43-52 cm	21	b.d.l.	35	b.d.l.
357-76B	10R1 U 91-111 cm	-	-	23	-29.5

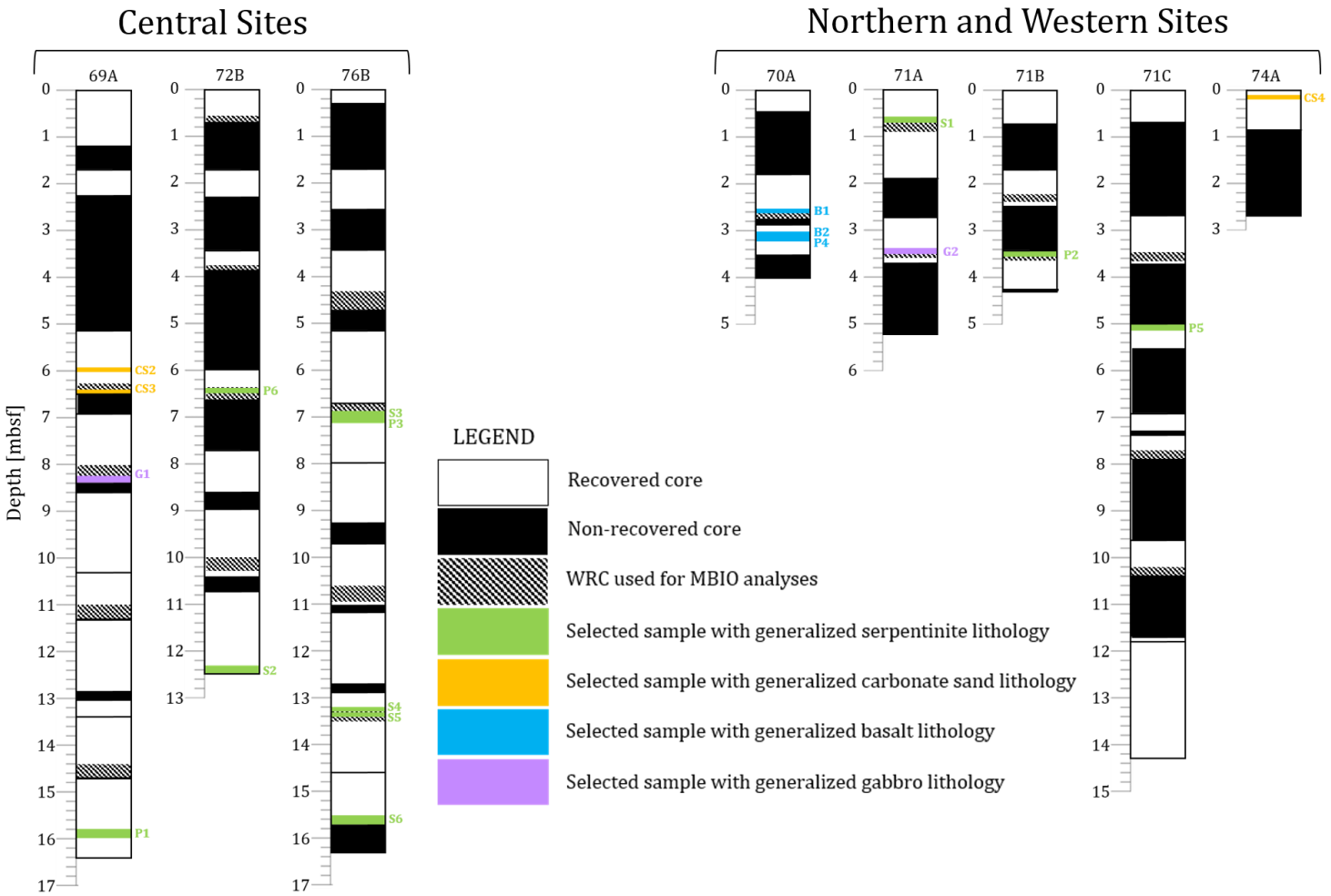

Figure 4.1 Core visualizations. Visualization of core depth comparisons and generalized lithology locations for each sample selected for organic matter analyses.

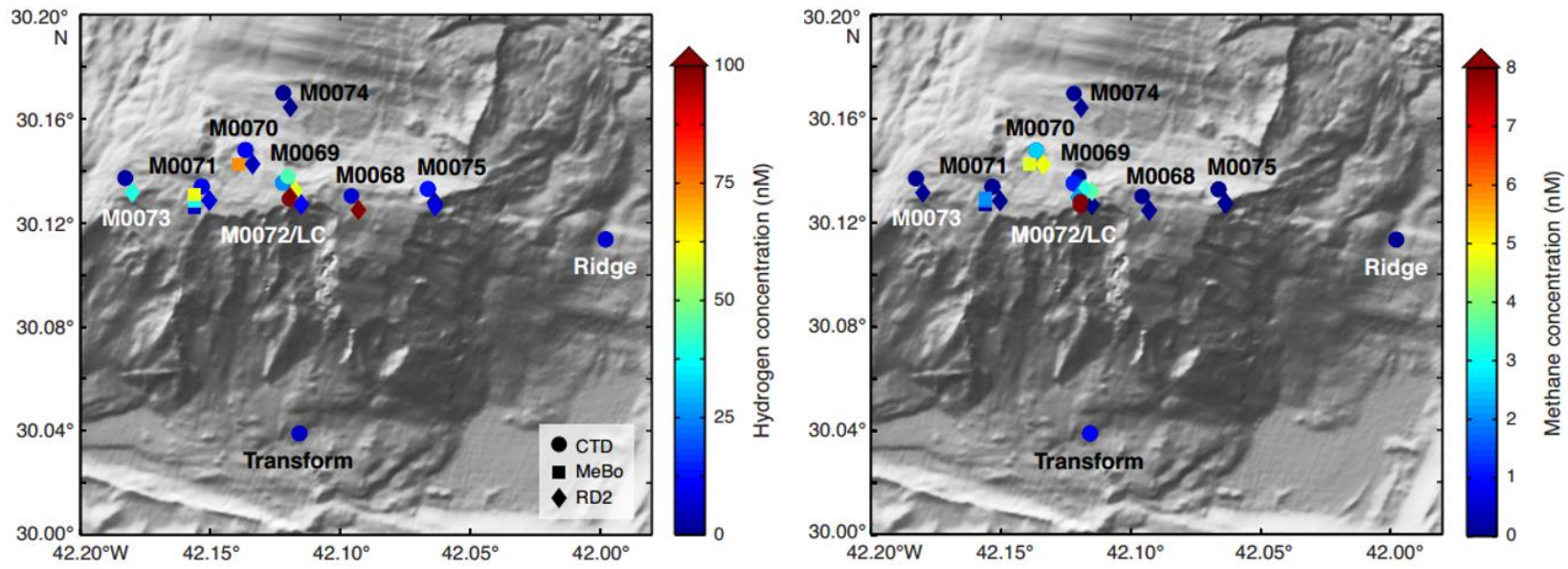

Figure 4.2 H_2 and CH_4 fluid concentrations. Dissolved H_2 and CH_4 in fluid samples across the Atlantis Massif. Figure reproduced from Früh-Green et al., 2017b.

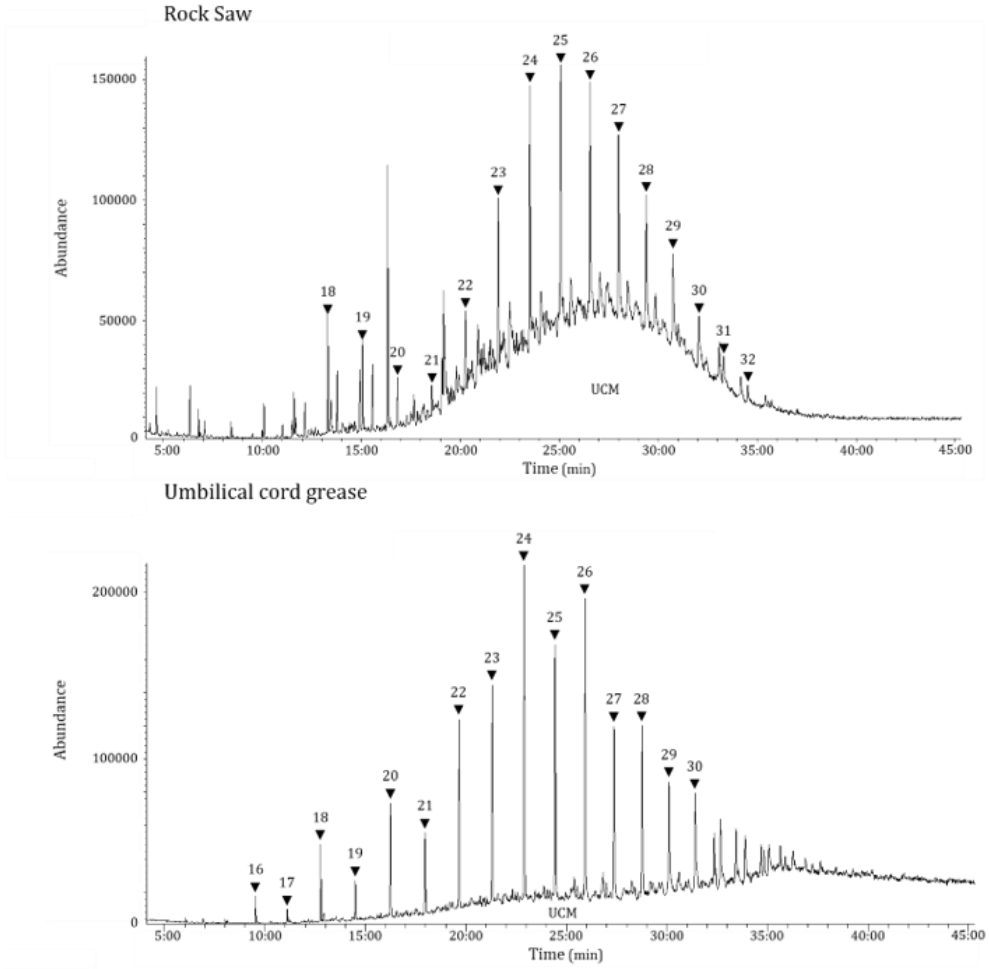

Figure 4.3 Rock saw and umbilical cord grease chromatograms. GC/MS chromatograms displaying the distribution of n-alkanes (marked with a ▼ with the corresponding number indicating the carbon number of the specific alkane) for the rock saw and umbilical cord grease contaminants.

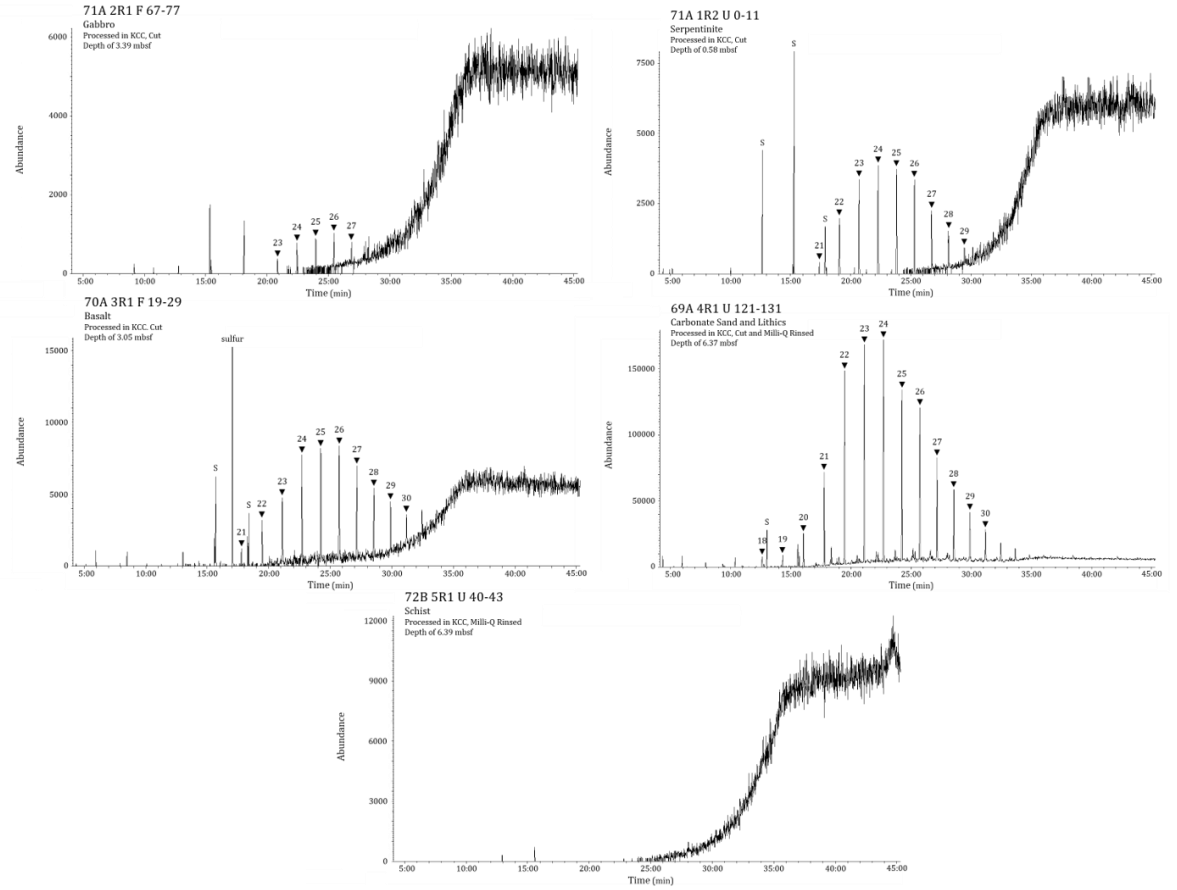

Figure 4.4 Expedition 357 sample chromatograms. GC/MS chromatograms displaying the distribution of n-alkanes (marked with a ▼ with the corresponding number indicating the carbon number of the specific alkane, S indicates siloxanes) in samples with various lithologies and processing types. Cut samples exhibited a characteristic n-alkane series ranging from C18 to C30 without the presence of any isoprenoidal biomarkers. The Milli-Q rinsed sample contained no detectable compounds.

CHAPTER 5

DISCUSSION

5.1 Steps to minimize contamination

Our interest in long-chain aliphatic compounds in subsurface rocks presented a unique challenge. To minimize external contamination and limit background signals, IODP drilling and sample processing procedures were, to the extent feasible, designed to maximize our ability to identify desired compounds without interference. Since all samples were to be shared between multiple PIs, additional steps were necessary to store samples in a manner appropriate for other analyses. For example, microbial culture experiments required maintaining anoxic conditions.

Prior to sampling, materials were tested for possible interference with lipid analysis. The bags used regularly to store core microbiological samples on the IODP vessel Chikyū (Escal Neo, GX-P film) contained high abundances of even n-alkanes and were deemed problematic for organic geochemical analyses, but had the benefit of keeping samples anoxic until they could be processed. Since acid-washed Teflon sheeting had a low contribution of lipid biomarkers, samples were first wrapped in this material then placed inside Escal Neo bags that were flushed

with N_2 and sealed. Nylon bags were found to be inappropriate for sample storage due to high contributions of amino acids, which could interfere with other future analyses (S. Lang, personal observations). The alkane series found in the core samples did not contain the even-over-odd carbon number predominance found in the Escal Neo bags, indicating that this compromise was effective in preventing contamination from the bags.

While all attempts were made to only touch the cores with the Teflon sheeting or cleaned metal instruments, it was at times necessary to touch the samples with gloved hands shipboard. Several different glove types were tested to identify those that would minimize the contribution of undesirable compounds. Three glove types were available at sea: Semperguard Xpert, VWR Nitrile 112-2373, and VWR Nitrile 112-2371. Semperguard Xpert gloves contained a large UCM peak but no identifiable alkanes and were therefore used at sea and at the Kochi Core Center during sample cutting and crushing. The KC500 purple nitrile gloves were used during all in-house extraction and separation procedures, though at this time it was never necessary to touch the sample directly and great care was taken to avoid contact between the gloves and the sample.

The outcome of these initial studies lead to the recommendation that upon arriving on deck, samples should be wrapped in acid-washed Teflon sheeting then stored in anoxic Escal Neo bags. This method was adopted by IODP Expedition

357. The lack of bag-derived alkanes and glove-derived UCM humps, plus clean lab processing blanks of combusted sand, suggested that these steps were largely effective.

5.2 No definitive evidence for biotically derived lipids

Archaea and bacteria produce distinct lipid biomarkers that can be used to identify their presence. Multiple microbiological and geochemical studies of the LCHF suggest methane-cycling archaea and sulfate reducing bacteria are the most likely microorganisms to be present in the Atlantis Massif subsurface (Schrenk et al., 2004; Brazelton et al., 2006). The 2,6,10,15,19-pentamethylicosane (PMI) compound is a highly specific biomarker produced by methanogenic and methanotrophic archaea (Peters et al., 2005) and has been found previously in the Lost City chimneys (Bradley et al., 2009). Hexadecanoic and octadecanoic acids are common fatty acids that indicate biological activity, while other more specific fatty acids, such as i17:1w7c and 10ME16:0, are also expressed by some sulfate-reducing bacteria (Peters et al., 2005; Dowling et al., 1988; Londry et al., 2004; Peters et al., 2005). It is possible that some of these lipids and fatty acids can exist in serpentinized rocks and be extracted and identified (Klein et al., 2015).

Examination of core sample chromatograms have indicated that there are no detectable isoprenoidal biomarkers amongst the n-alkane series. Previous

investigations of the Atlantis Massif, have identified isoprenoidal lipids such as phytane, pristane, norpristane, and squalane in rocks from both surface grab samples and subsurface cores (Delacour et al., 2008). The only unequivocally biological compounds present in the 357 samples were C_{16} and C_{18} fatty acids. Despite these compounds being biologically derived, they are ubiquitous and were identified in many potential contaminants used in this particular study. Therefore, the presence of theses fatty acids cannot be used to assess the existence and extent of a subsurface biosphere.

The lack of these diagnostic molecules did not outright confirm that these microorganisms are absent. Instead, these compounds could be below detection. Preliminary results from IODP collaborators have estimated the cell counts from similar samples to be $\approx 7.1 \times 10^3$ cells per cm^3 of rock with even lower estimates at greater depths (Früh-Green et al., 2017b). Our detection limit was approximately 1 ng of compound on column, and for our typical sample size of approximately 40 g, we would have needed approximately 10^5 cells per gram of rock to detect these compounds or sample sizes of 4 kilograms. The low cell counts from our samples compared to the number needed for detection could explain why no biomarkers were identified, despite alternative evidence for microbial activity in the serpentinite subsurface.

5.3 Source of the alkane series

Eleven core samples contained a similar series of straight-chain n-alkanes with an isotopic signature of -30.9‰ to -28.8‰. These compounds could have been derived from three potential sources: 1) biologically-derived from in situ microbial communities or the input of marine DOC, 2) abiotically-derived from FTT synthesis reactions, or 3) derived from contamination of different oils and greases used during samples drilling or processing.

5.3.1. Is the alkane series biologically derived?

This n-alkane series exhibited in the 357 rocks strongly resembled a similar distribution from previously collected serpentinites and gabbros from the Atlantis Massif (Delacour et al., 2008; Figure 2.2, Figure 4.4). This suite of compounds was previously attributed to sorption of marine DOC onto the rocks transported by high seawater fluxes through the massif (Delacour et al., 2008). The $\delta^{13}C$ isotopic values for the n-alkanes were similar between the two samples sets, suggesting that similar processes may be generating these compounds (Figure 5.1). The rocks from Expedition 357, however, lacked the previously observed isoprenoidal phytane, pristane, norpristane, and squalane biomarkers. It is therefore unlikely that the alkane series in our samples had a marine DOC source.

5.3.2. Is the alkane series abiotic?

Laboratory experiments examining the effects of serpentinization and FTT reactions have discovered specific trends that are indicative of abiotic compound synthesis. Abiogenic alkane distributions were characterized by a decrease in abundance as carbon number increases with no odd over even carbon number predominance (McCollom and Seewald, 2006; Figure 2.2b). The initial carbon source that was reacted with hydrogen to produce the alkane series generated different isotopic fractionation effects. When CO was used as the carbon source, n-alkanes (C_{15}-C_{30}) were approximately 28‰ more negative than the initial CO (McCollom et al., 2010). As these compounds are polymerized, the longer chain compounds had more positive isotopic signatures (McCollom et al., 2010). When formate was used as the carbon source, the alkanes were synthesized with a uniform isotopic fractionation of -30‰ (McCollom and Seewald, 2006; McCollom et al., 2010). Additional polymerization did not introduce a change in isotope values and there was minimal isotopic distinction between compounds (McCollom and Seewald, 2006; McCollom et al., 2010). No hydrocarbon polymerization was observed when CO_2 or CH_4 acted as the carbon source (McCollom and Seewald, 2006).

Similar to laboratory experiments, the alkane distribution exhibited in the basement rocks contained no carbon number predominance and decreased in

abundance with increasing carbon number. Also, the $\delta^{13}C$ isotopic values of our long-chain hydrocarbons remained uniform as carbon number increases, which was also observed in laboratory experiments with formate as a carbon source (Figure 5.2).

Formate concentrations are elevated in the Lost City fluids (Lang et al., 2010), which suggests that it is present in the subsurface and could be used as the carbon source for FTT reactions. With a -30‰ fractionation factor (McCollom and Seewald, 2006; McCollom et al., 2010), a formate $\delta^{13}C$ value of -0.9‰ to +1.2‰ would have been required to be the initial carbon source from which the Atlantis Massif alkanes were synthesized (-30.9‰ to -28.8‰). Formate in fluids from Lost City chimneys has recently been determined to consist of a mantle-derived source with a $\delta^{13}C$ of -12.7 ± -3.8‰ and a seawater derived source with a $\delta^{13}C$ of +8.4 ± 1.6‰ (Lang et al., submitted). It is, therefore, unlikely that alkanes synthesized from seawater-derived formate contributed to the observed n-alkane series, unless formate with a different isotopic composition is present away from the hydrothermal field. Further information on the carbon system of the Atlantis Massif and on experimentally-derived isotopic fractionation factors would help to constrain these possibilities.

5.3.3. Is the alkane series derived from contamination?

Sixteen grease, oil, and plastic samples that could have come into contact with the cores were also characterized for comparison to samples. The majority of tested contaminants did not contain the same saturated hydrocarbon distribution that was identified in the rock samples, but were rather composed of UCM humps or small distributions of even-numbered n-alkanes. The umbilical cord grease was the only shipboard contaminant with a chromatogram that contained the distinctive n-alkane signature that was analogous to what was observed in the rock samples. However, the umbilical cord grease n-alkane distribution had a minor even-over-odd carbon number predominance, which was not observed in the rock sample distribution (Figure 4.3). The $\delta^{13}C$ values of the umbilical cord grease n-alkanes (-31.7‰ to -30.8‰) were isotopically lighter than the $\delta^{13}C$ values of the rock sample alkanes (-30.9‰ to -28.8‰). Further, this grease was used only on one of the two rock drills, and was physically distant from the sample collection point, as it was used on the cable that lowered the drill to the seabed. It was therefore unlikely to be responsible for the n-alkanes observed in the samples.

The alkane concentrations were compared to a complementary study that used a chemical to tracer to assess sample contamination by drilling fluids. Perfluoromethylcyclohexane (PFC) was used as a tracer to qualify core contamination during seabed drilling (Früh-Green et al., 2017a; Orcutt et al., in prep). The PFC was introduced into the drilling fluid and, subsequently,

concentrations were measured in rock and fluid samples (Früh-Green et al., 2017a; Orcutt et al., in prep). The presence of PFC and, therefore, the intrusion of drilling fluid into the interior of the core, depended on core coherency (intact or rubbly), lithology, and processing style (Orcut et al., in prep). Regardless of borehole location, PFC concentrations were lower in the interiors of cores that were intact, did not contain veins, were not highly serpentinized (no talc), and were rinsed with Milli-Q water (Orcutt et al., in prep). The samples with the highest PFC abundances were not the same as the samples with highest alkane abundances. This implies that the drilling fluid, as identified by tracer intrusion, did not substantially contribute to the n-alkanes in the rock samples.

Samples processed by rock cutting contained the n-alkane series while those that were rinsed with Milli-Q water did not (Figure A.7). One possibility is that the rinse may have washed away loose phyllosilicate minerals which are expected to contain the highest concentrations of adsorbed organic molecules. This could have radically reduced the amount of organic compounds present in the sample. Alternatively, the n-alkane series could have been introduced to the eleven remaining samples whose exteriors were removed with a chilled rock saw despite extensive cleaning with methanol and RNase AWAY.

To test this possibility, potential contamination from the rock saw was assessed. A combusted filter dipped in methanol was then ran across the saw blade

and chilled plate. The extracts of these filters contained a series of n-alkanes that were identical to the distribution observed in our samples (Figures 4.3, 4.4). Subsequent $\delta^{13}C$ isotopic analysis of the rock saw hydrocarbons had values ranging from -31.0‰ to -30.1‰, indistinguishable from what was observed in the rock samples (-30.9‰ to -28.8‰). For example, the C_{24} alkane in the carbonate sand and lithics sample 69A 4R1 U 121-13 had a $\delta^{13}C$ isotopic signature of -30.6‰ with a corresponding $\delta^{13}C$ isotopic value of -30.9‰ in the rock saw. The hydrocarbon compounds found in the Atlantis Massif samples were therefore most likely sourced from the rock saw that was used to remove the core exteriors.

The Kochi Core Center rock saw was optimized to prevent microbiological contamination by being enclosed in a filtered air clean booth and cleaned with appropriate solvents but these steps were unfortunately not sufficient to fully remove contaminants. Minor contamination from a rock saw was recently implicated as the source of sterols in Archean rocks (French et al., 2015) that had previously been held as evidence for the rise of eukaryotes at ~2.7 Ga (Brocks et al., 1999). Even with solvent rinsing, the rock saw was a major source of biomarker contamination, in particular alkanes, steranes, and hopanes. There was also a strong correlation between the amount of hydrocarbons detected and the amount of newly sawed surface (French et al., 2015). Fully removing hydrocarbon contamination required heating the blade to 300°C for 1 hour and then

ultrasonicating it in a combusted aluminum foil envelope containing solvent (French et al., 2015).

Despite this result, it must be noted that the lack of a UCM hump in the Milli-Q rinsed sample chromatograms suggests that the sample processing and handling procedures implemented during this expedition were generally effective at eliminating surface or background contamination. Future research will undoubtedly focus on the detection of similar suites of compounds, particularly as drilling technology improves and increases recoveries in hard rock settings. Alternative methods to remove the exterior of rock cores should be explored. When doing so, consideration should simultaneously be given to preventing contamination for other analyses, such as microbiological studies, through assessment of possible contaminants to assess the source of compounds.

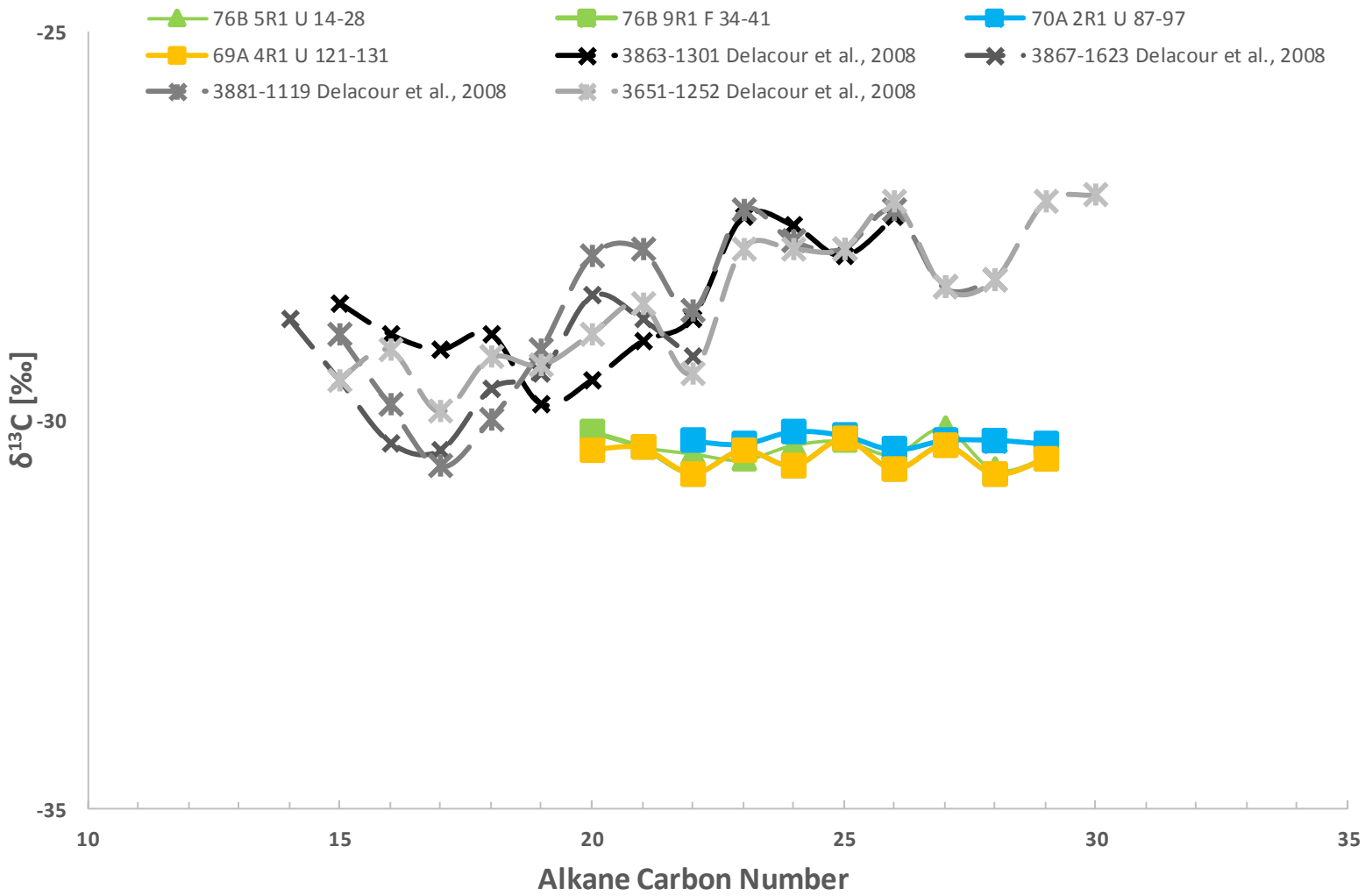

Figure 5.1 $\delta^{13}C$ isotopic values compared to biologically derived lipids. Comparison of $\delta^{13}C$ isotopic composition of sample alkanes to those determined by Delacour et al., 2008.

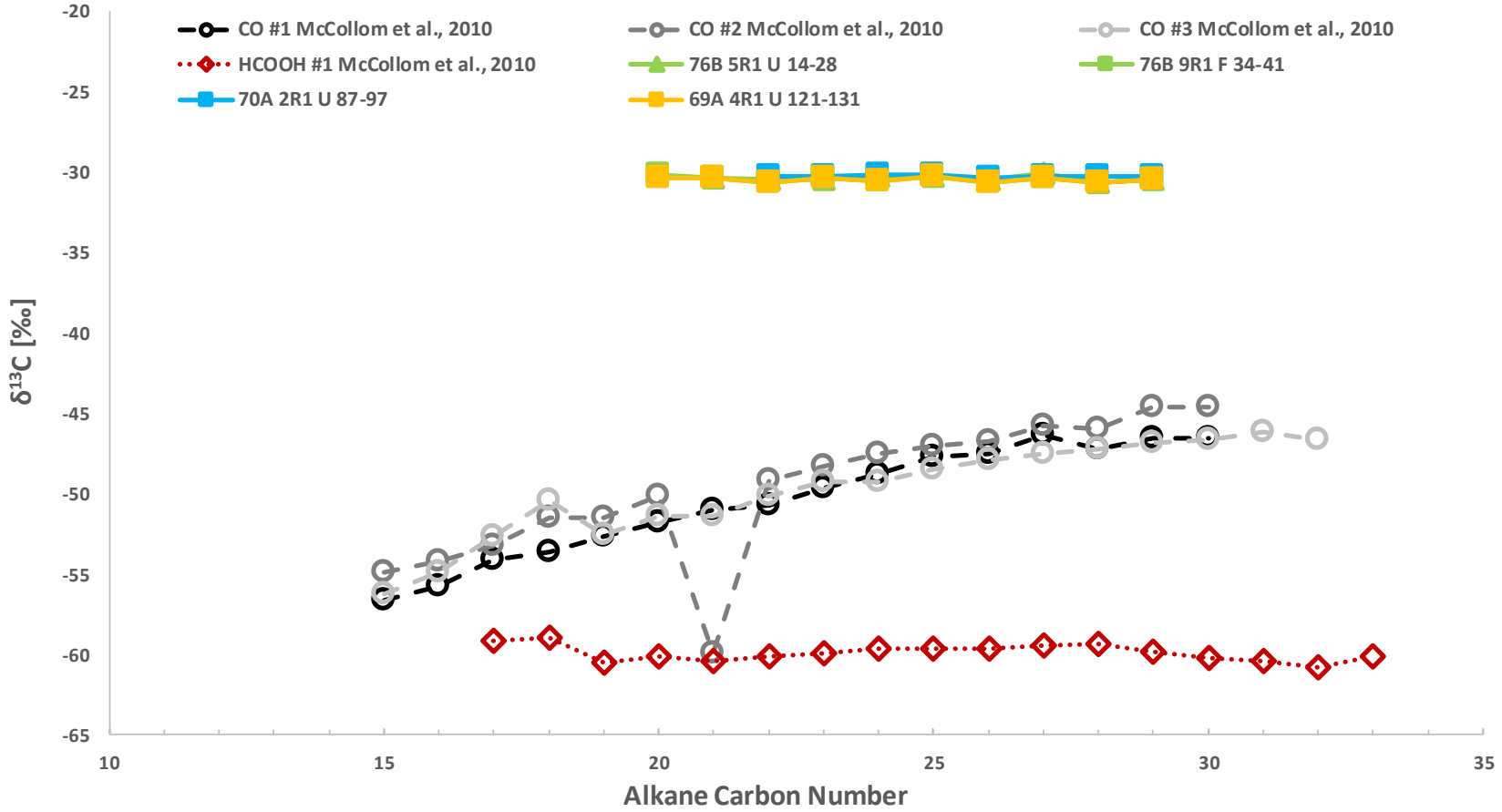

Figure 5.2 δ¹³C isotopic values compared to abiotically derived compounds. Comparison of δ¹³C isotopic composition of sample alkanes to those produced abiotically in lab experiments from CO and HCOOH from McCollom et al., 2010.

CHAPTER 6

CONCLUSIONS

The definitive detection and identification of abiotic and biological lipids in the subsurface of an actively serpentinizing system would be an important advance in understanding the development of pre-biotic chemistry and life in extreme environments. Accessing these environments requires complex drilling and processing procedures with numerous opportunities for contamination to occur. Microbiologists working with these tools in low biomass environments have been particularly focused on minimizing and characterizing potential contamination. They have lead the development of chemical, microbiological, and particulate tracers in an attempt to quantify contamination throughout the entire drilling process (Smith et al., 2000; Lever et al., 2006; D'Hondt et al., 2007; Santelli et al., 2010; Frise et al., 2017; Orcutt et al., in prep). For example, methods involving PFC tracers and fluorescent microspheres have been extensively implemented to measure the intrusion of drilling fluids and nonindigenous microorganisms, respectively, into drilled cores (Lever et al., 2006; Orcutt et al., in prep). However, many significant microbiological and geochemical discoveries using ODP drilled

rock or sediment cores have been claimed without explicitly discussing the possibility of contamination (Smith et al., 2000).

Similar issues face studies of lipid biomarkers and other organic compounds in subsurface environments. As highlighted in the study of French et al., (2015), it is difficult to ascertain whether previous conclusions made using subsurface lipid biomarkers accurately represent in situ processes without in depth characterization of contaminants. Such characterization is necessary to avoid ambiguity concerning any future conclusions made using deep biosphere organic compounds. However, as demonstrated in this study, the simple adoption of contamination techniques developed primarily for tracking cells is not sufficient when sample analyses focus on lipids.

Biologically derived compounds could not be definitively identified in the Atlantis Massif samples, indicating that any active biosphere in the serpentinite subsurface is present at levels below our detection limits. The cores recovered from the subsurface contained a series of C_{18} to C_{30} n-alkanes with ^{13}C signatures of -30.9‰ to -28.8‰. These straight-chain hydrocarbons were only identified in samples that had their exteriors removed with a rock saw rather than being rinsed with Milli-Q water. The similarity in alkane distributions and isotope signatures between samples and swipes of the rock saw implicate the rock saw as the source of these compounds. While it is possible that abiotically-derived compounds could

have been present, it was impossible to identify any due to contamination. This result highlights the critical importance of minimizing and thoroughly characterizing potential contamination at all steps along the sample processing pathway in order to prevent misinterpretation.

Despite contaminant-derived compounds being present in our cut samples, the remaining cores did not contain the same alkane contamination. This suggests that many of the steps taken to prevent contamination were effective and should be implemented in future endeavors. It provides some optimism for detecting compounds in future drilling projects despite the difficulties inherent in completely eliminating contamination during drilling. However, we advise caution in the use of a rock saw to remove core exteriors. Harsher cleaning methods than solvent cleaning are necessary to remove organics from the blade. The potential loss of material during Milli-Q rinsing also make this approach somewhat problematic. Alternative mechanisms could be more successful, such as chipping away the exterior of samples or implementing the cleaning procedures of French et al. (2015). These approaches should be thoroughly tested prior to and during implementation and, similar to the requirements for microbiological studies, future publications should include the results of these assessments.

Detecting lipid biomarkers in serpentinites will continue to be a goal for researchers interested in the development of pre-biotic chemistry and the survival

of life in the subseafloor. As this research progresses, methodological improvements to the minimization and characterization of potential contaminants should also occur.

REFERENCES

Ammannito, E., De Sanctis, M.C., Ciarniello, M., Frigeri, A., Carrozzo, F.G., Combe, J.-Ph., Ehlmann, B.L., Marchi, S., McSween, H.Y., Raponi, A., Toplis, M.J., Tosi, F., Castillo-Rogez, J.C., Capaccioni, F., Capria, M.T., Fonte, S., Giardino, M., Jaumann, R., Longobardo, A., Joy, S.P., Magni, G., McCord, T.B., McFadden, L.A., Palomba, E., Pieters, C.M., Polanskey, C.A., Rayman, M.D., Raymond, C.A., Schenk, P.M., Zambon, F., Russell, C.T., 2016. Distribution of phyllosilicates on the surface of Ceres. Science 353, aaf4279.

Barnes, I., LaMarche Jr., V.C., Himmelberg, G., 1967. Geochemical evidence of present-day serpentinization. Science 156, 830-832.

Barnes, I., O'Neil, J.R., Trescases, J.J., 1978. Present day serpentinization in New-Caledonia, Oman and Yugoslavia. Geochimica et Cosmochimica Acta 42, 144–145.

Blackman, D.K., Karson, J.A., Kelley, D.S., Cann, J.R., Früh-Green, G.L., Gee, J.S., Hurst, S.D., John, B.E., Morgan, J., Nooner, S.L., Foss, D.K., Schroeder, T.J., Williams, E.A., 2002. Geology of the Atlantis Massif (Mid-Atlantic Ridge, 30°N): Implications for the evolution of an ultramafic core complex. Marine Geophysical Researches 23, 443-469.

Bradley, A.S., Hayes, J.M., Summons, R.E., 2009. Extraordinary C-13 Enrichment of diether lipids at the Lost City Hydrothermal Field indicates a carbon-limited system. Geochimica et Cosmochimica Acta 73, 102-118.

Brazelton, W.J., Schrenk, M.O., Kelley, D.S., Baross, J.A., 2006. Methane- and sulfur-metabolizing microbial communities dominate the Lost City Hydrothermal Field ecosystem. Applied and Environmental Microbiology 72, 6257-6270.

Brazelton, W.J., Mehta, M.P., Kelley, D.S., Baross, J.A., 2011. Physiological differentiation within a single-species biofilm fueled by serpentinization. mBio 2, 1-9.

Brocks J.J., Logan, G.A., Buick, R., Summons, R.E., 1999. Archean molecular fossils and the early rise of eukaryotes. Science 285, 1033-1036.

Combe, J.-Ph., McCord, T.B., Tosi, F., Ammannito, E., Carrozzo, F.G., De Sanctis, M.C., Raponi,A., Byrne, S., Landis, M.E., Hughson, K.H.G., Raymond, C.A., Russell, C.T., 2016. Detection of local H_2O exposed at the surface of Ceres. Science 353, aaf3010.

D'Hondt, S., Inagaki, F., Ferdelman, T., JØrgensen, B.B., Kato, K., Kemp, P., Sobecky, P., Sogin, M., and Takai, K., 2007. Workshop report: Exploring subseafloor life with the Integrated Ocean Drilling program. Sci. Drilling, 5:26-37.

De Sanctis, M.C., Ammannito, E., Raponi, A., Marchi, S., McCord, T.B., McSween, H.Y., Capaccioni, F., Capria, M.T., Carrozzo, F.G., Ciarniello, M., Longobardo, A., Tosi, F., Fonte, S., Formisano, M., Frigeri, A., Giardino, M., Magni, G., Palomba, E., Turrini, D., Zambon, F., Combe, J.-Ph., Feldman, W., Jaumann, R., McFadden, L.A., Pieters, C.M., Prettyman, T., Toplis, M., Raymond, C.A., Russell, C.T., 2015. Ammoniated phyllosilicates with a likely outer Solar System origin on (1) Ceres. Nature 528, 241–244.

De Sanctis, M.C., Raponi, A., Ammannito, E., Ciarniello, M., Toplis, M.J., McSween, H.Y., Castillo-Rogez, J.C., Ehlmann, B.L., Carrozzo, F.G., Marchi, S., Tosi, F., Zambon, F., Capaccioni, F., Capria, M.T., Fonte, S., Formisano, M., Frigeri, A., Giardino, M., Longobardo, A., Magni, G., Palomba, E., McFadden, L.A., Pieters, C.M., Jaumann, R., Schenk, P., Mugnuolo, R., Raymond, C.A., Russell, C.T., 2016. Bright carbonate deposits as evidence of aqueous alteration on (1) Ceres. Nature 536, 54–57.

De Sanctis, M.C., Ammannito, E., McSween, H.Y., Raponi, A., Marchi, S., Capaccioni, F., Capria, M.T., Carrozzo, F.G., Ciarniello, M., Fonte, S., Formisano, M., Frigeri, A., Giardino, M., Longobardo, A., Magni, G., McFadden, L.A., Palomba, E., Pieters, C.M., Tosi, F., Zambon, F., Raymond, C.A., Russell, C.T., 2017. Localized aliphatic organic material on the surface of Ceres. Science 355, 719-722.

Delacour, A., Früh-Green, G.L., Bernasconi S.M., Schaeffer, P., Kelley D.S., 2008. Carbon geochemistry of serpentinites in the Lost City Hydrothermal System (30°N, MAR). Geochimica et Cosmochimica Acta 72. 3681-3702.

Dowling, N.J.E., Nichols, P.D., White, D.C., 1988. Phospholipid fatty acid and infra-red spectroscopic analysis of a sulphate-reducing consortium. FEMS Microbiology Letters 53, 325-333.

Eickmann, B., Bach, W., Rosner, M., Peckman, J., 2009a. Geochemical constraints on the modes of carbonated precipitation in peridotites from the Logatchev Hydrothermal Vent Field and Gakkel Ridge. Chemical Geology 268, 97-106.

Eickmann, B., Bach, W., Peckman, J., 2009b. Authigenesis of Carbonate Minerals in Modern and Devonian Ocean-Floor Hard Rocks. The Journal of Geology 117, 307-323.

Foustoukos, D.I., Seyfried Jr., W.E., 2004. Hydrocarbons in hydrothermal vent fluids: the role of chromium-bearing catalysts. Science 304, 1002-1005.

French, K.L., Hallmann, C., Hope, J.M., Schoon, P.L., Zumberge, J.A., Hoshino, Y., Peters, C.,A., George, S.C., Love, G.D., Brocks, J.J., Buick, R., Summons, R.E., 2015. Reappraisal of hydrocarbon biomarkers in Archean rocks. PNAS 112, 5915-5920.

Frise, A., Kallmeyer, J., Kitte, J.A., Martinez, I.M., Bijaksana, S., Wagner, D., ICP Lake Chalco Drilling Science Team, ICDP Towuti Drilling Science Team, 2017. A simple inexpensive technique for assessing contamination during drilling operations. Limnology and Oceanography Methods 15: 200-211.

Früh-Green, G.L., Kelley, D.S., Bernasconi, S.M., Karson, J.A., Ludwig, K.A., Butterfield, D.A., Boschi, C., Proskurowski, G., 2003. 30,000 years of hydrothermal activity at the Lost City Vent Field. Science 301, 495-498.

Früh-Green, G.L., Connolly, J.A.D., Plas, A., Kelley, D.S., Groberty, B., 2004. Serpentinization of oceanic peridotites: Implications for geochemical cycles and biological activity, In: Wilcock, W.D., DeLong, E.F., Kelley, D.S., Baross, J.A., Cary, S.C. (Eds.), Geophysical Monograph Series 144. American Geophysical Union, Washington, DC, pp 119-136.

Früh-Green, G., Andreani, M., Baross, J., Bernasconi, S., Boschi, C., Brazelton, W., Cannat, M., Cheadle, M., Delacour, A., Escartin, J., Godard, M., Gouze, P., Holm, N., Ildefonse, B., Ivarsson, M., John, B., Kelley, D., Lang, S., Lilley, M., MacLeod, C., McCaig, A., Menez, B., Morris, A., Schrenk, M., Searle, R., 2010. Proposal #758: Serpentinization and Life: Biogeochemical and tectono-magmatic processes in young mafic and ultramafic seafloor. International Ocean Discovery Program.

Früh-Green, G., Orcutt, B.N., Green, S.L., Cotterill, C., Morgan, S., Akizawa, N., Bayrakci, G., Behrmann, J.-H., Boschi, C., Brazelton, W.J., Cannat, M., Dunkel, K.G., Escartín, J., Harris, M., Herrero-Bervera, E., Hesse, K., John, B.E., Lang, S.Q., Lilley, M.D., Liu, H.Q., Mayhew, L.E., McCaig, A.M., Menez, B., Morono, Y., Quéméneur, M., Rouméjon, S., Sandaruwan Ratnayake, A., Schrenk, M.O., Schwarzenbach, E.M., Twing, K., Weis, D., Whattham, S.A., Williams, M., Zhao, R., 2017a. Expedition 357 summary, In: Früh-Green, G.L., Orcutt, B.N., Green, S.L., Cotterill, C., and Scientists, E. (Eds.), Atlantis Massif Serpentinization and Life. Proceedings of the International Ocean Discovery Program, 357, International Ocean Discovery Program, College Station, TX.

Früh-Green, G., Orcutt, B.N., Green, S.L., Cotterill, C., Morgan, S., Akizawa, N., Bayrakci, G., Behrmann, J.-H., Boschi, C., Brazelton, W.J., Cannat, M., Dunkel, K.G., Escartín, J., Harris, M., Herrero-Bervera, E., Hesse, K., John, B.E., Lang, S.Q., Lilley, M.D., Liu, H.Q., Mayhew, L.E., McCaig, A.M., Menez, B., Morono, Y., Quéméneur, M., Rouméjon, S., Sandaruwan Ratnayake, A., Schrenk, M.O., Schwarzenbach, E.M., Twing, K., Weis, D., Whattham, S.A., Williams, M., Zhao, R., 2017b. Eastern sites, In: Früh-Green, G.L., Orcutt, B.N., Green, S.L., Cotterill, C., and Scientists, E. (Eds.), Atlantis Massif Serpentinization and Life. Proceedings of the International Ocean Discovery Program, 357, International Ocean Discovery Program, College Station, TX.

Greene, J.A., Tominaga, M., Blackman, D.K., 2015. Geologic implications of seafloor character and carbonate lithification imaged on the domal core of Atlantis Massif. Deep-Sea Research II 121, 246-255.

Hedges, J.I., 1977. The association of organic molecules with clay minerals in aqueous solutions. Geochimica et Cosmochimica Acta 41, 1119-1123.1

Horita, J., Berndt, M.E., 1999. Abiogenic methane formation and isotopic fractionation under hydrothermal conditions. Science 285, 1055-1057.

Karson, J.A., Früh-Green, G.L., Kelley, D.S., William, E.A., Yoerger, D.R., and Jakuba, M., 2006. Detachment shear zone of the Atlantis Massif core complex, Mid-Atlantic Ridge, 30°N. Geochemistry, Geophysics, Geosystems 7, Q06016.

Kelley, D.S., Karson, J.A., Blackman, D.K., Früh-Green, G.L., Butterfield, D.A., Lilley, M.D., Olson, E.J., Schrenk, M.O., Roe, K.K., Lebon, G.T., Rivizzigno, P., AT3-60 Shipboard Party, 2001. An off-axis hydrothermal vent field near the Mid-Atlantic Ridge at 30°N. Nature 412, 145-149.

Kelley, D.S., Karson, J.A., Früh-Green, G.L., Yoerger, D.R., Shank, T.M., Butterfield, D.A., Hayes, J.M., Schrenk, M.O., Olson, E.J., Proskurowski, G., Jakuba, M., Bradley, A., Larson, B., Ludwig, K., Glickson, D., Buckman, K., Bradley, A.S., Brazelton, W.J., Roe, K., Elend, M.J., Delacour, A., Bernasconi, S.M., Lilley, M.D., Baross, J.A., Summons, R.E., Sylva, S.P., 2005. A serpentinite-hosted ecosystem: the Lost City Hydrothermal Field. Science 307, 1428-1434.

Klein, F., Humphris, S.E., Guo, W., Schubotz, F., Schwarzenbach, E.M., Orsi, W.D., 2015. Fluid mixing and the deep biosphere of a fossil Lost-City type hydrothermal system at the Iberia Margin. PNAS Early Edition 112, 12036-12041.

Lang, S.Q., Butterfield, D.A., Schulte, M., Kelley, D.S., Lilley, M.D., 2010. Elevated concentrations of formate, acetate and dissolved organic carbon found at the Lost City hydrothermal field. Geochimica et Cosmochimica Acta 74, 941-952.

Lang, S.Q., Früh-Green, G.L., Bernasconi, S.M., Lilley, M.D., Proskurowski, G., Méhay, S., Butterfield, D.A., 2012. Microbial utilization of abiogenic carbon and hydrogen in a serpentinite-hosted system. Geochimica et Cosmochimica Acta 92, 82-99.

Lang, S.Q., Früh-Green, G.L., Bernasconi, S.M., Brazelton, W.J., Schrenk, M.O., and McGonigle, J.M., (submitted) Deeply-sourced formate fuels sulfate reducers but not methanogens at Lost City hydrothermal field.

Londry, K.L., Jahnke, L.L., Des Marais, D.J., 2004. Stable carbon isotope ratios of lipid biomarkers of sulfate-reducing bacteria. Applied and Environmental Microbiology 70, 745-751.

Ludwig, K.A., Kelley, D.S., Butterfield, D.A., Nelson, B.K., Früh-Green, G.L., 2006. Formation and evolution of carbonate chimneys at the Lost City Hydrothermal Field. Geochimica et Cosmochimica Acta 70, 3625-3645.

Ludwig, K.A., Shen, C.-C., Kelley, D.S., Cheng, H., Edwards, R.L., 2011. U–Th systematics and ^{230}Th ages of carbonate chimneys at the Lost City Hydrothermal Field. Geochimica et Cosmochimica Acta 75, 1869-1888.

Malamud, U., Prialnik, D., 2013. Modeling serpentinization: Applied to the early evolution of Enceladus and Mimas. Icarus 225, 763-774.

Martin, W., Russell, M.J., 2003. On the origin of cells: a hypothesis for the evolutionary transitions from abiotic geochemistry to chemoautotrophic prokaryotes and from prokaryotes to nucleated cells. Philosophical Transactions of the Royal Society-B 358, 59-85.

Masui, N., Morono, Y., and Inagaki, F., 2009. Bio-archive core storage and subsampling procedure for subseafloor molecular biological research. Sci. Drilling, 8, 35-37.

McCollom, T.M., Seewald, J.S., 2006. Carbon isotope composition of organic compounds produced by abiotic synthesis under hydrothermal conditions. Earth and Planetary Science Letters 243, 74-84.

McCollom, T.M., 2007a. Geochemical constraints on sources of metabolic energy for chemolithoautotrophy in ultramafic-hosted deep-sea hydrothermal systems. Astrobiology 7, 933-950.

McCollom, T.M., Seewald, J.S., 2007b. Abiotic synthesis of organic compounds in deep-sea hydrothermal environments. Chemical Reviews 107, 382-401.

McCollom, T.M., Lollar, B.S., Lacrampe-Couloume, G., Seewald, J.S., 2010. The influence of carbon source on abiotic organic synthesis and carbon isotope fractionation under hydrothermal conditions. Geochimica et Cosmochimica Acta 74, 2717-2740.

Méhay, S., Früh-Green, G.L., Lang, S.Q., Bernasconi, S.M., Brazelton, W.J., Schrenk, M.O., Schaeffer, P., Adam, P., 2013. Record of archaeal activity at the serpentinite-hosted Lost City Hydrothermal Field. Geobiology 11, 570-592.

Moody, J.B., 1976. Serpentinization: a review. Lithos 9, 125-138.

Nozaka, T., Fryer, P., Andreani, M., 2008. Formation of clay minerals and exhumation of lower-crustalrocks at Atlantis Massif, Mid-Atlantic Ridge. Geochemistry, Geophysics, Geosystems 9, Q11005.

Niemann, H.B., Atreya, S.K., Bauer, S.J., Carignan, G.R., Demick, J.E., Frost, R.L., Gautier, D., Haberman, J.A., Harpold, D.N., Hunten, D.M., Israel, G., Lunine, J.I., Kasprzak, W.T., Owen, T.C., Paulkovich, M., Raulin, F., Raaen, E., Way, S.H., 2005. The abundances of constituents of Titan's atmosphere from the GCMS instrument on the Huygens probe. Nature 438, 779–784.

Orcutt, B.N., Bergenthal, M., Freudenthal, T., Smith, D., Lilley, M.D., Schneiders, L., Früh-Green, G.L., (in prep). Contamination tracer testing with seabed drills: IODP Expedition 357. Scientific Drilling.

Oze C., Sharma, M., 2005. Have olivine, will gas: Serpentinization and the abiogenic production of methane on Mars. Geophysical Research Letters 32, L10203.

Pearson, V.K., Sephton, M.A., Kearsley A.T., Bland, P.A., Franchi, I.A., Gilmour I., 2002. Clay mineral-organic matter relationships in the early solar system. Meteoritics & Planetary Science 37, 1829-1833.

Peters, K.E., Walters, C.C., Moldowan, J.M., 2005. The Biomarker Guide II 2nd Edition: Biomarkers and Isotopes in Petroleum Systems and Earth History. Cambridge University Press, UK.

Proskurowski, G., Lilley, M.D., Seewald, J.S., Früh-Green, G.L., Olson, E.J., Lupton, J.E., Sylva, S.P., Kelley, D.S., 2008. Abiogenic hydrocarbon production at Lost City Hydrothermal Field. Science 319, 604-607.

Schrenk, M.O., Kelley, D.S., Bolton, S.A., Baross, J.A., 2004. Low archeal diversity linked to subseafloor geochemical processes at the Lost City Hydrothermal Field, Mid-Atlantic Ridge. Environmental Microbiology 6, 1086-1095.

Schrenk, M.O., Huber, J.A., Edwards, K.J., 2010. Microbial provinces in the subseafloor. Annual Review of Marine Science 2, 279-304.

Schrenk, M.O., Brazelton, W.J., Lang, S.Q., 2013. Serpentinization, carbon, and deep life. Reviews in Mineralogy & Geochemistry 75, 575-606.

Schwarzenbach, E.M., Lang, S.Q., Früh-Green, G.L., Lilley, M.D., Bernasconi, S.M., Méhay, S., 2013. Sources and cycling of carbon in continental, serpentinite-hosted alkaline springs in the Voltri Massif, Italy. Lithos 177, 226-244.

Sherwood Lollar, B., Westgate, T.D., Ward, J.A., Slater G.F., Lacrampe-Couloume, G., 2002. Abiogenic formation of alkanes in the Earth's crust as a minor source for global hydrocarbon reservoirs. Nature 416, 522-524.

Shock, E.L., Schulte, M.D., 1998. Organic synthesis during fluid mixing in hydrothermal systems. Journal of Geophysical Research 103, 28513-28527.

Smith, D.C., Spivack, A.J., Fisk, M.R., Haveman, S.A., Staudigel, H., 2000. Tracer-based estimates of drilling-induced microbial contamination of deep sea crust. Geomicrobiology Journal 17, 207-219.

Sleep, N.H., Bird, D.K., Pope, E.C., 20ll. Serpentinite and the dawn of life. Philosophical Transactions of the Royal Society B 366, 2857–2869.

Suzuki, S., Ishii, S., Wu, A., Cheung, A., Tenney, A., Wanger, G., Kuenen, G., Nealson, K.H., 2013. Microbial diversity in The Cedars, an ultrabasic, ultrareducing, and low salinity serpentinizing ecosystem. PNAS 110, 15336-15341.

Tobie, G., Lunine, J.I., Sotin, C., 2006. Episodic outgassing as the origin of atmospheric methane on Titan. Nature 440, 61–64.

Yanagawa, K., Nunoura, T., McAllister, S.M., Hirai, M., Breuker, A., Brandt, L., House, C.H., Moyer, C.L., Birrien, J.-L., Aoike, K., Sunamura, M., Urabe, T., Mottl, M.J., Takai, K., 2013. The first microbiological contamination assessment by deep-sea drilling and coring by the D/V Chikyu at the Iheya

North hydrothermal field in the Mid-Okinawa Trough (IODP Expedition 331). Frontiers in Microbiology 4, 1-10.

APPENDIX A

SUPPLEMNTAL INFORMATION

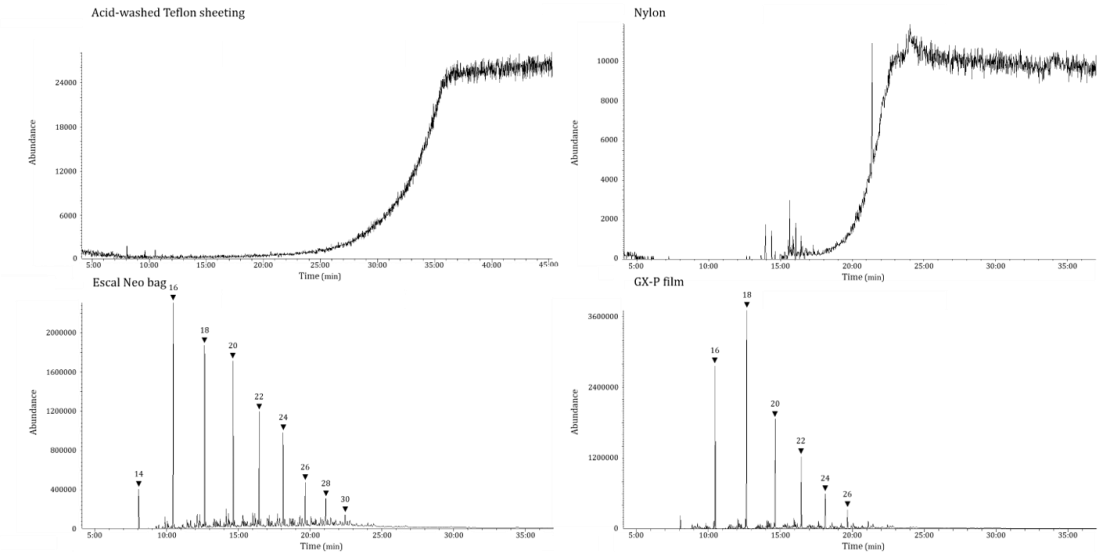

Figure A.1 Contaminant chromatograms: bags. GC/MS chromatograms displaying the distribution of n-alkanes (marked with a ▼ with the corresponding number indicating the carbon number of the specific alkane, S indicates siloxanes) in cut serpentinites samples.

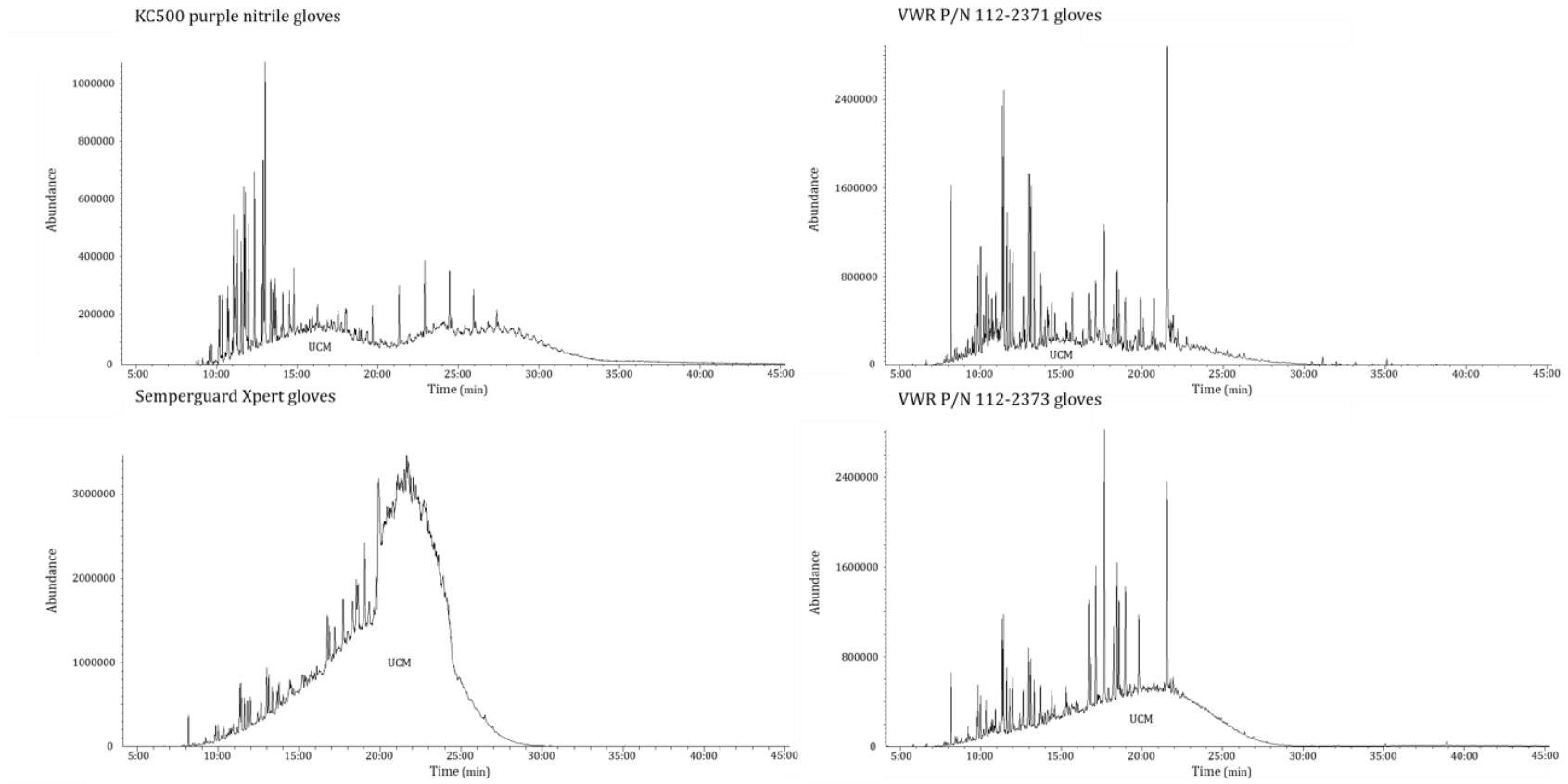

Figure A.2 Contaminant chromatograms: gloves. GC/MS chromatograms displaying the saturated hydrocarbon distribution (UCM denotes unresolved complex mixture) in 4 glove samples. Two grams of each glove type underwent the extraction procedure and out of 25 μL of sample dissolved in hexane, 1 μL was injected into the GC-MS and GC-C-IRMS.

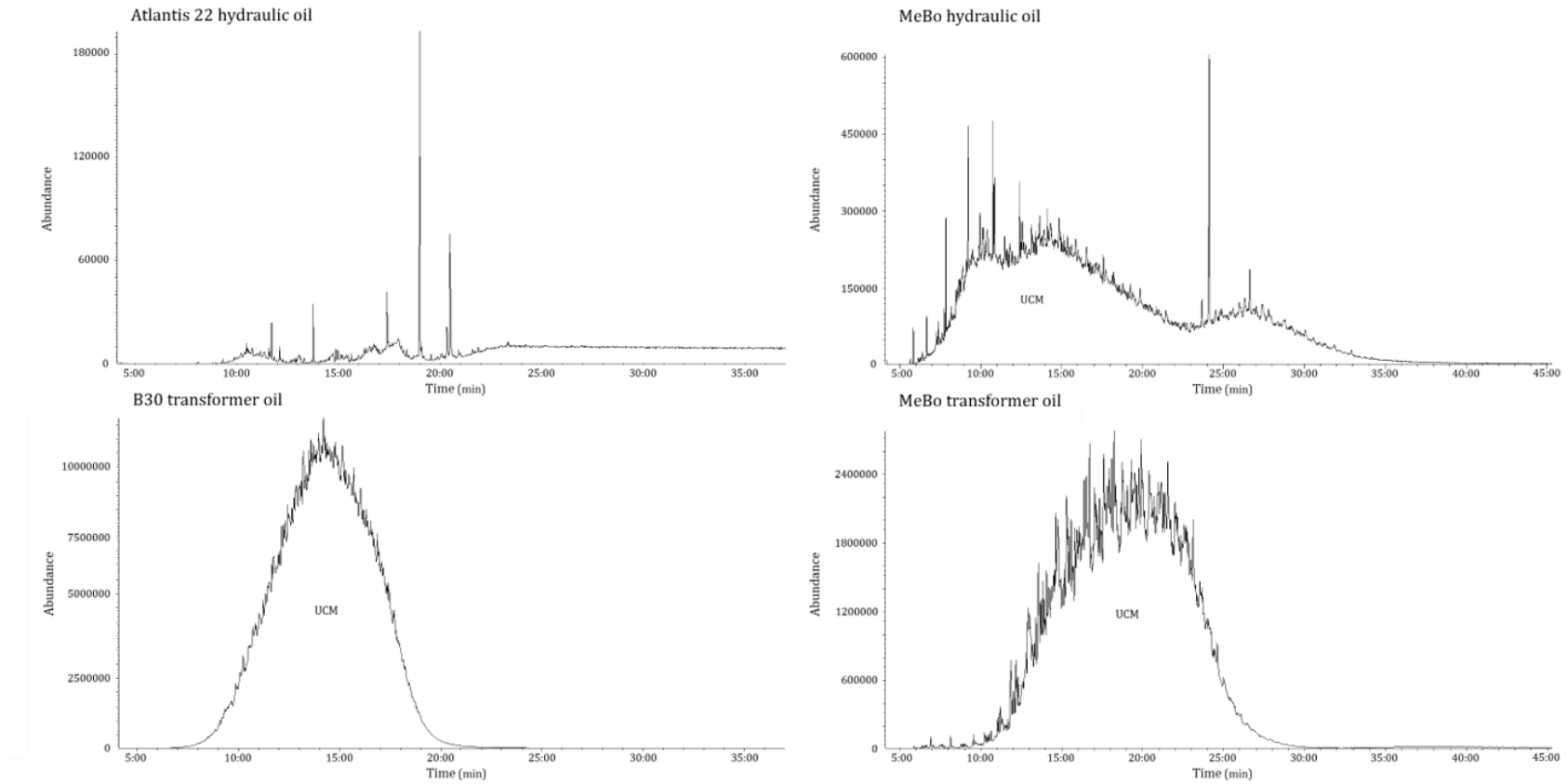

Figure A.3 Contaminant chromatograms: oils. GC/MS chromatograms displaying the saturated hydrocarbon distribution (UCM denotes unresolved complex mixture) in 5 oil and grease samples. N-alkanes marked with a ▼ with the corresponding number indicating the carbon number of the specific alkane.

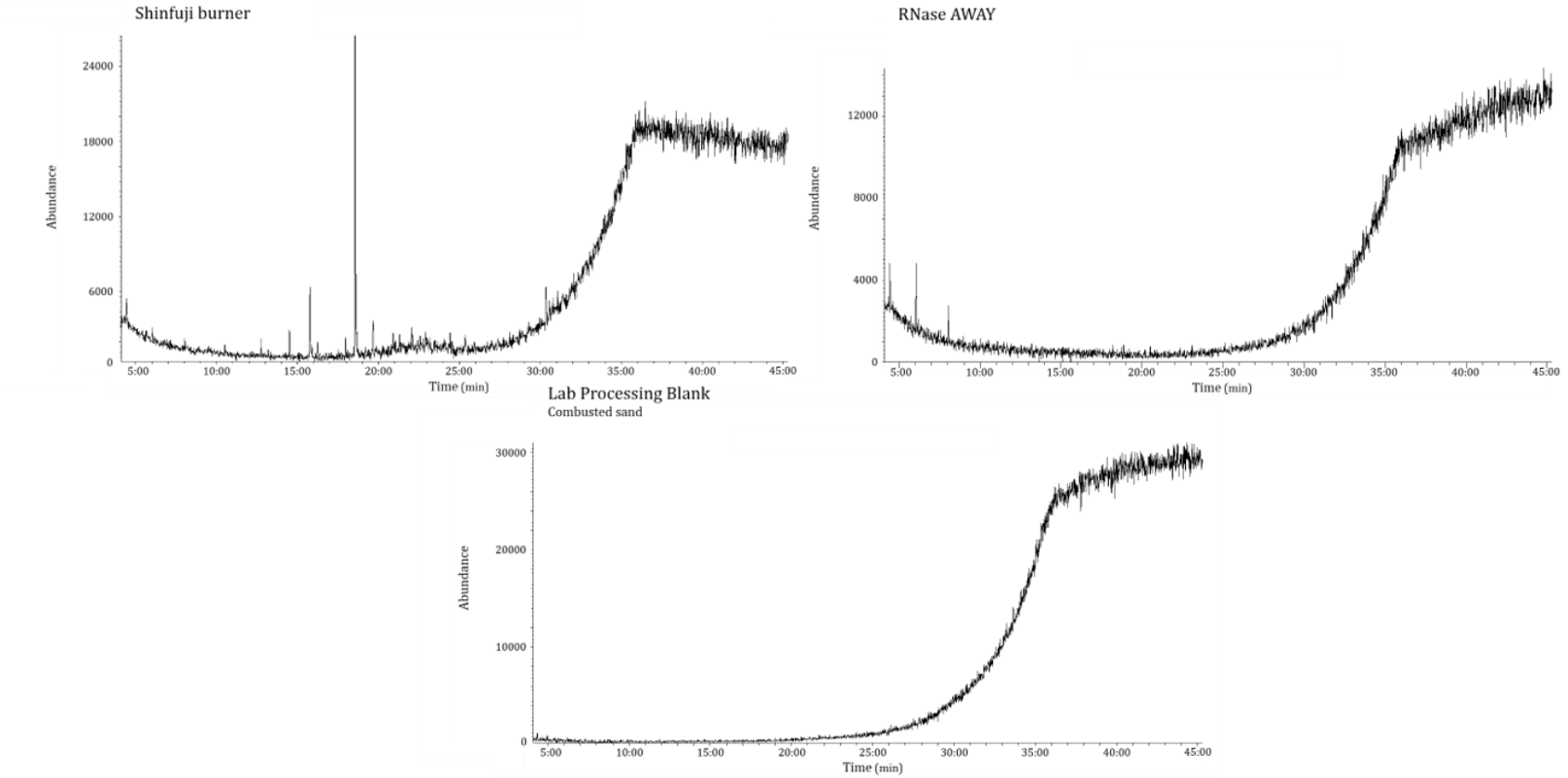

Figure A.4 Contaminant chromatograms: Shinfuji burner, RNase AWAY. GC/MS chromatograms displaying the saturated hydrocarbon distribution in Shinfuji burner, RNase AWAY, and the combusted sand lab processing blank.

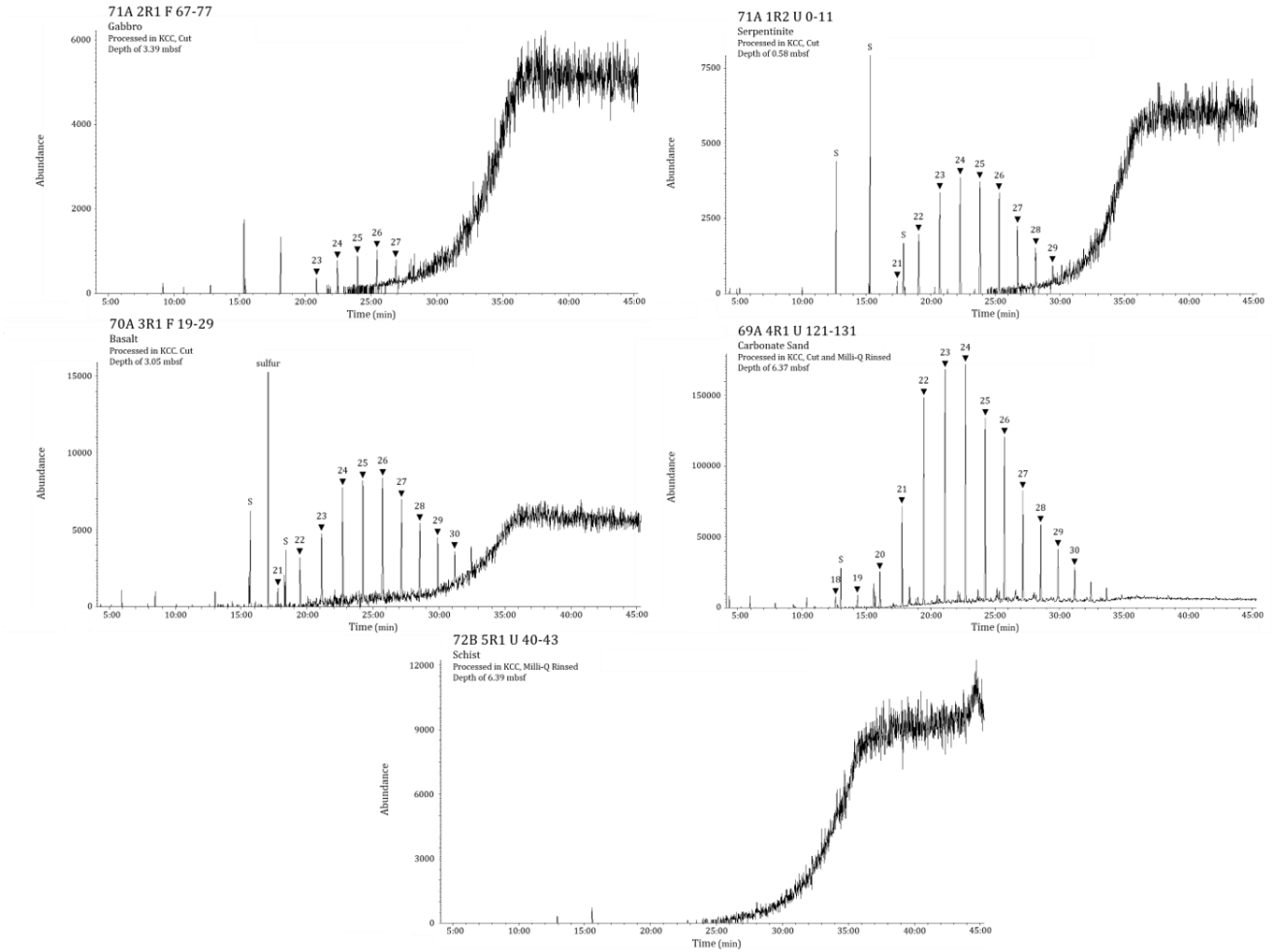

Figure A.5 Expedition 357 chromatograms: cut serpentinites. GC/MS chromatograms displaying the distribution of n-alkanes (marked with a ▼ with the corresponding number indicating the carbon number of the specific alkane, S indicates siloxanes) in cut serpentinites samples.

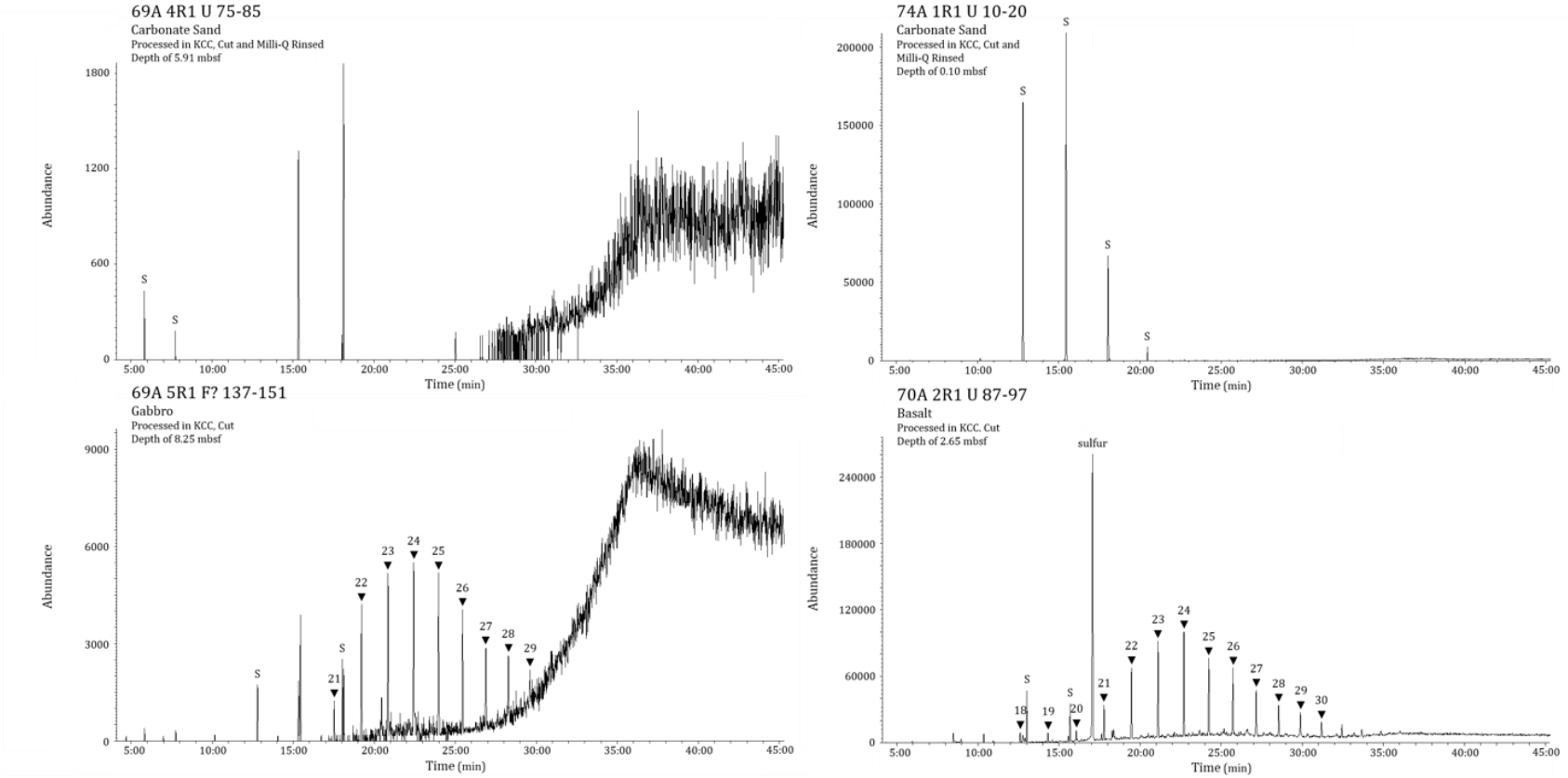

Figure A.6 Expedition 357 chromatograms: cut samples. GC/MS chromatograms displaying the distribution of n-alkanes (marked with a ▼ with the corresponding number indicating the carbon number of the specific alkane, S indicates siloxanes) in cut samples with various lithologies.

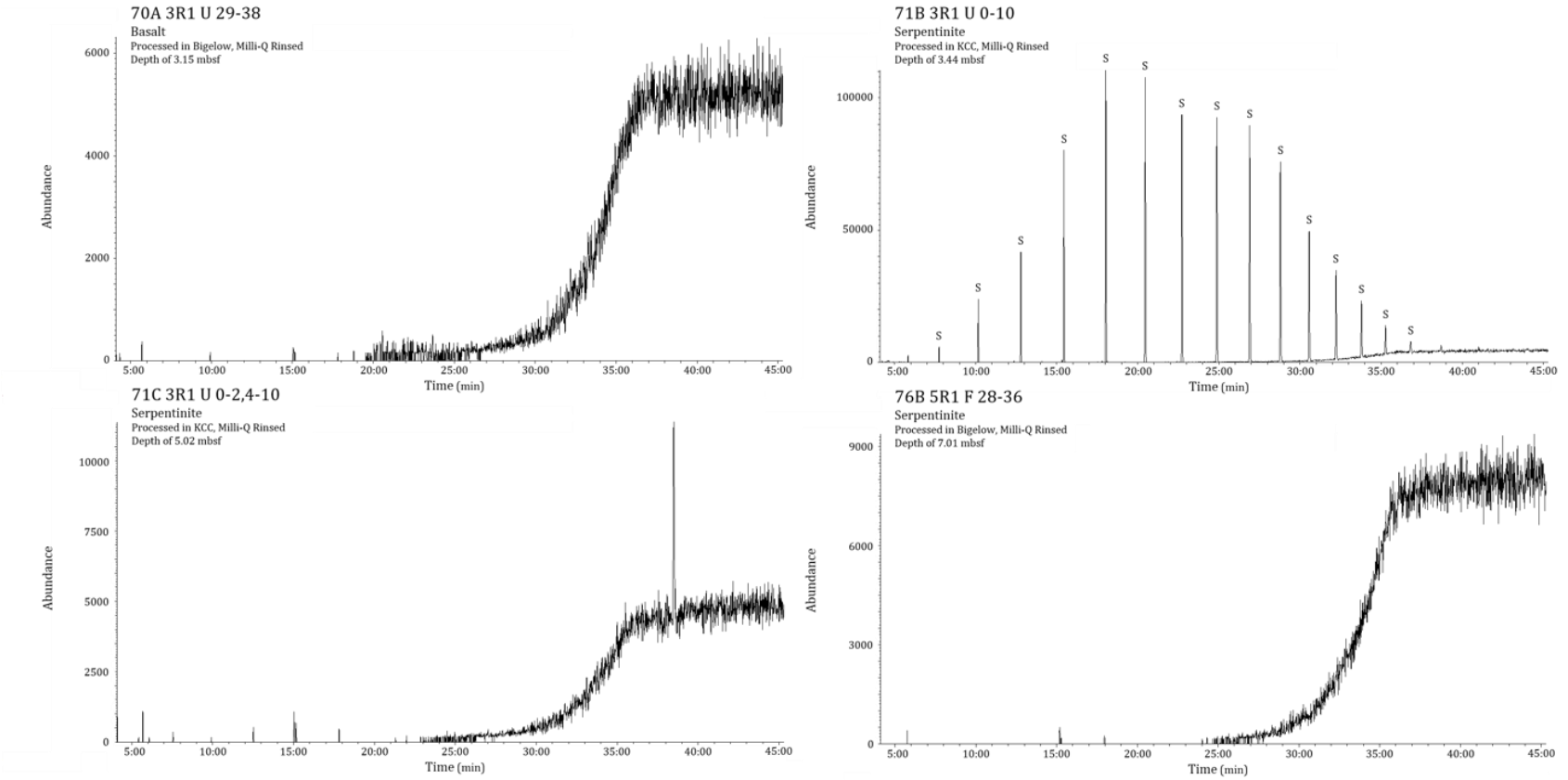

Figure A.7 Expedition 357 chromatograms: Milli-Q rinsed samples. GC/MS chromatograms displaying the distribution of n-alkanes (marked with a ▼ with the corresponding number indicating the carbon number of the specific alkane, S indicates siloxanes) in Milli-Q rinsed samples with various lithologies.